

# Macroeconomic Dynamics Near the ZLB: A Tale of Two Countries \*

S. Boragan Aruoba

*University of Maryland*

Pablo Cuba-Borda

*Federal Reserve Board*

Frank Schorfheide

*University of Pennsylvania*

*CEPR and NBER*

First Version: September 10, 2012

Current Version: December 9, 2016

## Abstract

We compute a sunspot equilibrium in an estimated small-scale New Keynesian model with a zero lower bound (ZLB) constraint on nominal interest rates and a full set of stochastic fundamental shocks. In this equilibrium a sunspot shock can move the economy from a regime in which inflation is close to the central bank's target to a regime in which the central bank misses its target, inflation rates are negative, and interest rates are close to zero with high probability. A nonlinear filter is used to examine whether the U.S. in the aftermath of the Great Recession and Japan in the late 1990s transitioned to a deflation regime. The results are somewhat sensitive to the model specification, but on balance, the answer is affirmative for Japan and negative for the U.S.

JEL CLASSIFICATION: C5, E4, E5

KEY WORDS: Deflation, DSGE Models, Japan, Multiple Equilibria, Nonlinear Filtering, Nonlinear Solution Methods, Sunspots, U.S., ZLB

---

\* Correspondence: B. Aruoba: Department of Economics, University of Maryland, College Park, MD 20742. Email: aruoba@econ.umd.edu. P. Cuba-Borda: Division of International Finance, Federal Reserve Board, 20th Street & Constitution Ave., NW, Washington, DC 20551. Email: pablo.a.cubaborda@frb.gov. F. Schorfheide: Department of Economics, 3718 Locust Walk, University of Pennsylvania, Philadelphia, PA 19104. Email: schorf@ssc.upenn.edu. This paper previously circulated under the title "Macroeconomic Dynamics Near the ZLB: A Tale of Two Equilibria". We are thankful for helpful comments and suggestions from the editor, the referees, Saroj Bhattarai, Jeff Campbell, John Cochrane, Hiroshi Fujiki, Hidehiko Matsumoto, Karel Mertens, Morten Ravn, Stephanie Schmitt-Grohe, Mike Woodford, and participants of various conferences and seminars. Much of this paper was written while Aruoba and Schorfheide visited the Federal Reserve Bank of Philadelphia, whose hospitality they are thankful for. Aruoba and Schorfheide gratefully acknowledge financial support from the National Science Foundation under grants SES 1061725 and 1424843. The views expressed in this paper are solely the responsibility of the authors and should not be interpreted as reflecting the views of the Board of Governors of the Federal Reserve System or of anyone else associated with the Federal Reserve System.

# 1 Introduction

Japan has experienced near-zero interest rates and a deflation of about -1% since the late 1990s. In the U.S. the federal funds rate dropped below 20 basis points in December 2008 and has stayed near zero in the aftermath of the Great Recession through the end of 2015. Investors' access to currency, which yields a zero nominal return, prevents interest rates from falling below zero and thereby creates a zero lower bound (ZLB) for nominal interest rates. The recent experiences of the U.S. and Japan have raised concern among policy makers about a long-lasting switch to a regime in which interest rates are zero, inflation is low, and conventional macroeconomic policies are less effective. For instance, in the aftermath of the Great Recession the president of the Federal Reserve Bank of St. Louis, James Bullard wrote: "During this recovery, the U.S. economy is susceptible to negative shocks that may dampen inflation expectations. This could push the economy into an unintended, low nominal interest rate steady state. Escape from such an outcome is problematic. [...] The United States is closer to a Japanese-style outcome today than at any time in recent history." (Bullard (2010))

The key contribution of this paper is to provide the first formal econometric analysis of the likelihood that the U.S. and Japan have transitioned to a long-lasting zero interest rate and low inflation regime. Starting point is a standard small-scale New Keynesian dynamic stochastic general equilibrium (DSGE) model. We explicitly impose the ZLB constraint on the interest rate feedback rule. We assume that in normal times monetary policy is active in the sense that the central bank changes interest rates more than one-for-one in response to deviations of inflation from the target. Moreover, fiscal policy is assumed to be passive in the sense that the fiscal authority uses lump-sum taxes to balance the government budget constraint in every period. It is well known that in such an environment there are two steady states. In the targeted-inflation steady state, inflation equals the value targeted by the central bank and nominal interest rates are strictly positive. In the second steady state, the deflation steady state, nominal interest rates are zero and inflation rates are negative.<sup>1</sup>

---

<sup>1</sup>The second steady state is often called *undesirable*. However, in the context of a standard New Keynesian DSGE model with an explicit money demand motive, this steady state is not necessarily bad in terms of welfare. While negative inflation rates in conjunction with a cost of adjusting nominal prices lead to an

To assess the likelihood of a transition to a deflation regime, we construct a stochastic equilibrium, in which agents react to fundamental shocks (e.g., technology shocks, demand shocks, monetary policy shocks) as well as to a Markov-switching sunspot shock that can move the economy between a targeted inflation regime and a deflation regime.<sup>2</sup> This equilibrium offers two potential explanations for the recent experiences in the U.S. and Japan: the economies may have been pushed to the ZLB either by a sequence of adverse fundamental shocks in the targeted-inflation regime or by a switch to the deflation regime. The type of explanation has important implications, not just for the central bank's ability to stimulate the economy using conventional interest rate policies, but also for the effectiveness of fiscal policy, as documented in Mertens and Ravn (2014). Aggregating results from different model specifications, we find that Japan shifted from the targeted-inflation regime into the deflation regime in 1999 and remained there until the end of our sample. The U.S., in contrast, remained in the targeted-inflation regime throughout its ZLB episode, with the possible exception of the first part of 2009, where the evidence is more mixed.

More specifically, using a first-order perturbation approximation of the targeted-inflation regime, we estimate six DSGE model specifications for each country that differ in terms of interest rate feedback rule, exogenous shocks, and observables used in the estimation. Once the parameter estimates are obtained, we work directly with the nonlinear sunspot equilibrium. At a technical level, our paper is the first paper to use global projection methods to compute a sunspot equilibrium for a DSGE model with a full set of stochastic shocks that can be used to track macroeconomic time series.

In order to identify the regime (targeted-inflation versus deflation) for each model specification, we use a particle filter to extract the sequence of shocks that can explain the data. Most importantly, we obtain estimates of the probability that the economies were in either of the two regimes. We find that for the U.S. five out of six specifications indicate that a switch to the deflation regime was very unlikely. For Japan, the regime probabilities are

---

output loss, the zero interest rate implies that the welfare losses arising from the opportunity cost of holding real money balances are eliminated. We leave a careful normative analysis to future work.

<sup>2</sup>Cass and Shell (1983) define sunspots as extrinsic uncertainty that does not affect tastes, endowments, or production possibilities. Sunspot shocks can affect economic outcomes in environments in which there does not exist a unique equilibrium; see Benhabib and Farmer (1999) for a review.

more sensitive to the model specification. Four of the specifications imply that there is a high probability that Japan spent most of the time in the deflation regime since the late 1990s. Finally, we aggregate the results based on quasi posterior model probabilities that we obtain using predictive likelihood scores for the set of observables that is common across specifications (output, inflation, and interest rates). Weighing the evidence, we conclude that there is a very high probability that Japan has switched to the deflation regime sometime in the late 1990s and that the U.S. remained in the targeted-inflation regime throughout its ZLB episode.

Our paper is related to three strands of the literature: multiplicity of equilibria in New Keynesian DSGE models; global projection methods for the solution of DSGE models; and the use of particle filters to extract hidden states in nonlinear DSGE models.

There has been extensive research on multiplicity of equilibria in New Keynesian DSGE models generated by so-called passive monetary policy rules that do not respond strongly enough to inflation deviations from target. Such policy rules are associated with undetermined local fluctuations in the neighborhood of the targeted-inflation steady state. An econometric analysis of this type of multiplicity is provided by Lubik and Schorfheide (2004). If monetary policy is active instead of passive then the local dynamics near the targeted-inflation steady state are unique (subject to the caveats emphasized in Cochrane (2011)). On the other hand, in the neighborhood of the deflation steady state, the central bank is unable to lower interest rates in response to a drop in inflation and thus the local dynamics are indeterminate.<sup>3</sup> Benhabib et al. (2001a,b) were the first to construct equilibria in which the economy transitions from the targeted-inflation steady state toward the deflation steady state. Recently, Armenter (2014) generalizes their results to a model in which monetary policy is not represented by a Taylor rule, but it is optimally chosen to maximize social welfare.

It should be clear from the above discussion that the model considered in our analysis has many equilibria. This opens the door for two research strategies: (i) characterize as many equilibria as possible and then examine which of these equilibria is consistent with the

---

<sup>3</sup>Hirose (2014) estimates a linearized New Keynesian DSGE model by imposing that the economy is permanently at the ZLB and parameterizing the multiplicity of solutions as in Lubik and Schorfheide (2004).

data. (ii) Choose one particular equilibrium and condition the empirical analysis on that equilibrium. The papers by Lubik and Schorfheide (2004) (studying inflation and interest rate dynamics before and after the Volcker disinflation) and Cochrane (2015) (studying inflation and interest rate dynamics during a ZLB episode and a subsequent exit from the ZLB) consider linearized DSGE models and are examples of the first approach. Our paper pursues the second avenue: we consider a particular equilibrium within which we can address the question of whether an economy has transitioned into a long-lasting deflation regime. While there are other equilibria that allow for similar transitions, yet might exhibit different regime-conditional dynamics, at present it is computationally not feasible to enumerate. Thus, we focus our empirical analysis on an interesting equilibrium for which we do have a solution.

A sunspot equilibrium similar to ours has been analyzed by Mertens and Ravn (2014), but in a model with a much more restrictive exogenous shock structure. Schmitt-Grohé and Uribe (2015) study an equilibrium in which confidence shocks, which resemble a change in regimes in our model, combined with downward nominal wage rigidity can deliver jobless recoveries near the ZLB in a mostly analytical analysis. Piazza (2016) shows that different monetary policy rules may change the path from the targeted-inflation steady state to the deflation steady state and demonstrates in a calibrated model that a combination of a perfect-foresight sunspot shock and a shock to the growth rate of the economy can generate dynamics similar to the Japanese experience. Our paper is the first to compute a sunspot equilibrium in a New Keynesian DSGE model that is rich enough to track macroeconomic time series.

In terms of solution method, our work is most closely related to the papers by Judd et al. (2010), Maliar and Maliar (2015), Fernández-Villaverde et al. (2015), and Gust et al. (2012).<sup>4</sup> All of these papers use global projection methods to approximate agents' decision rules in a New Keynesian DSGE model with a ZLB constraint. However, these papers solely

---

<sup>4</sup>Most of the other papers that study DSGE models with a ZLB constraint take various shortcuts to solve the model. In particular, following Eggertsson and Woodford (2003), many authors assume that an exogenous Markov-switching process pushes the economy to the ZLB. The subsequent exit from the ZLB is exogenous and occurs with a prespecified probability. The absence of other shocks makes it impossible to use the model to track actual data. Unfortunately, model properties tend to be very sensitive to the approximation technique and to implicit or explicit assumptions about the probability of leaving the ZLB, see Boneva et al. (2016) and Fernández-Villaverde et al. (2015).

consider an equilibrium in which the economy is always in the targeted-inflation regime – what we could call a targeted-inflation equilibrium – and some important details of the implementation of the solution algorithm are different.

With respect to the empirical analysis, the only other papers that combine a projection solution with a nonlinear filter to track U.S. data throughout the Great Recession period are Gust et al. (2012) and Cuba-Borda (2014). Both papers restrict their attention to the targeted-inflation equilibrium. The first focuses on parameter estimation using post-2008 data in a New Keynesian model like ours and examine the extent to which the ZLB constrained the ability of monetary policy to stabilize the economy. The latter extracts fundamental shocks to account for the decline in economic activity during the U.S. Great Recession in a medium-scale model with investment. Our paper is the first to fit a nonlinear DSGE model with an explicit ZLB constraint to Japanese data.

The remainder of the paper is organized as follows. Section 2 presents a simple two-equation model that we use to illustrate the multiplicity of equilibria in monetary models with ZLB constraints. We also highlight the particular equilibrium studied in this paper. The New Keynesian model that is used for the quantitative analysis is presented in Section 3, and the solution of the model is discussed in Section 4. Section 5 describes the parameter estimates for the different model specifications in this paper and illustrates the dynamic properties of one of the estimated model specifications. Section 6 presents our main results regarding the identification of the sunspot regime in each country. Section 7 concludes. Detailed derivations, descriptions of algorithms, and additional quantitative results are summarized in an Online Appendix.

## 2 A Two-Equation Example

We begin with a simple two-equation example to characterize the sunspot equilibrium that we will study in the remainder of this paper. Suppose that the economy can be described

by a consumption Euler equation of the form

$$1 = \mathbb{E}_t \left[ M_{t+1} \frac{R_t}{\pi_{t+1}} \right] \quad (1)$$

and a monetary policy rule

$$R_t = \max \left\{ 1, r\pi_* \left( \frac{\pi_t}{\pi_*} \right)^\psi \right\}, \quad \psi > 1, \quad (2)$$

where  $r$  is the steady state gross real interest rate,  $R_t$  is the gross nominal interest rate,  $\pi_t$  is the gross inflation rate, and  $\pi_*$  is the target of the central bank for the gross inflation rate. The subsequent analysis is based on the assumption the monetary policy is active in the sense that  $\psi > 1$ , which is the prevailing view of U.S. monetary policy after the Volcker disinflation. We assume that the gross nominal interest rate is bounded from below by one, which is captured by the max operator in (2). Throughout the paper we refer to this bound as the ZLB because the net interest rate cannot fall below zero.

In the fully-specified DSGE model introduced in Section 3 below, the stochastic discount factor  $M_{t+1}$  that appears in (1) is given by

$$M_{t+1} = \beta \frac{d_{t+1}}{d_t} \left( \frac{C_{t+1}}{C_t} \right)^{-\tau},$$

where  $C_t$  is consumption,  $d_t$  is a discount factor shock, and  $1/\tau$  is the intertemporal elasticity of substitution. To keep the example simple, we assume that  $M_t$  is exogenous and follows a stationary AR(1) process

$$\log \left( \frac{M_{t+1}}{m} \right) = \rho \log \left( \frac{M_t}{m} \right) + \sigma \epsilon_{t+1}, \quad \epsilon_{t+1} \sim iidN(0, 1) \text{ and } \rho \in (0, 1). \quad (3)$$

The parameter  $m$  is the steady state ( $\sigma = 0$ ) of the stochastic discount factor and equals  $1/r$ .

Loglinearizing around  $\pi_t = \pi_*$ ,  $M_t = 1/r$  and  $R_t = r\pi_*$ , and using hats to denote

percentage deviations from this point, yields the system

$$\hat{R}_t = \mathbb{E}_t \left[ -\hat{M}_{t+1} + \hat{\pi}_{t+1} \right] \quad (4)$$

$$\hat{R}_t = \max \{ -\log(r\pi_*) , \psi\hat{\pi}_t \} \quad (5)$$

$$\hat{M}_{t+1} = \rho\hat{M}_t + \sigma\varepsilon_{t+1} \quad (6)$$

where (4) is a version of the Fisher equation, which relates the nominal interest rate to the expected real interest rate and inflation. A similar system of equations arises from the log-linearized equilibrium conditions of many monetary DSGE models. Combining (4) and (5) and using  $\mathbb{E}_t[\hat{M}_{t+1}] = \rho\hat{M}_t$  yields the following expectational difference equation for inflation

$$\mathbb{E}_t [\hat{\pi}_{t+1}] = \max \{ -\log(r\pi_*) + \rho\hat{M}_t, \psi\hat{\pi}_t + \rho\hat{M}_t \}. \quad (7)$$

Just as the original system comprising (1) and (2), the difference equation (7) has two steady states. In the targeted-inflation steady state inflation equals  $\pi_*$ , and the nominal interest rate is  $R_* = r\pi_*$ , so that  $\hat{\pi} = \hat{R} = 0$ . In the deflation steady state,  $\hat{\pi} = \hat{R} = -\log(r\pi_*)$  and thus inflation equals  $1/r$ , and the nominal interest rate is at the ZLB.

The presence of two steady states suggests that the rational expectations difference equation (7) also has multiple stochastic solutions. We find solutions to this equation using a guess-and-verify approach (see the Online Appendix for details). Suppose that we conjecture

$$\hat{\pi}_t = \theta_0 - \theta_1 \hat{M}_t. \quad (8)$$

It can be verified that a solution that fluctuates around the targeted-inflation steady state (henceforth targeted-inflation equilibrium) is given by<sup>5</sup>

$$\theta_0^* = 0, \quad \theta_1^* = \frac{\rho}{\psi - \rho} > 0. \quad (9)$$

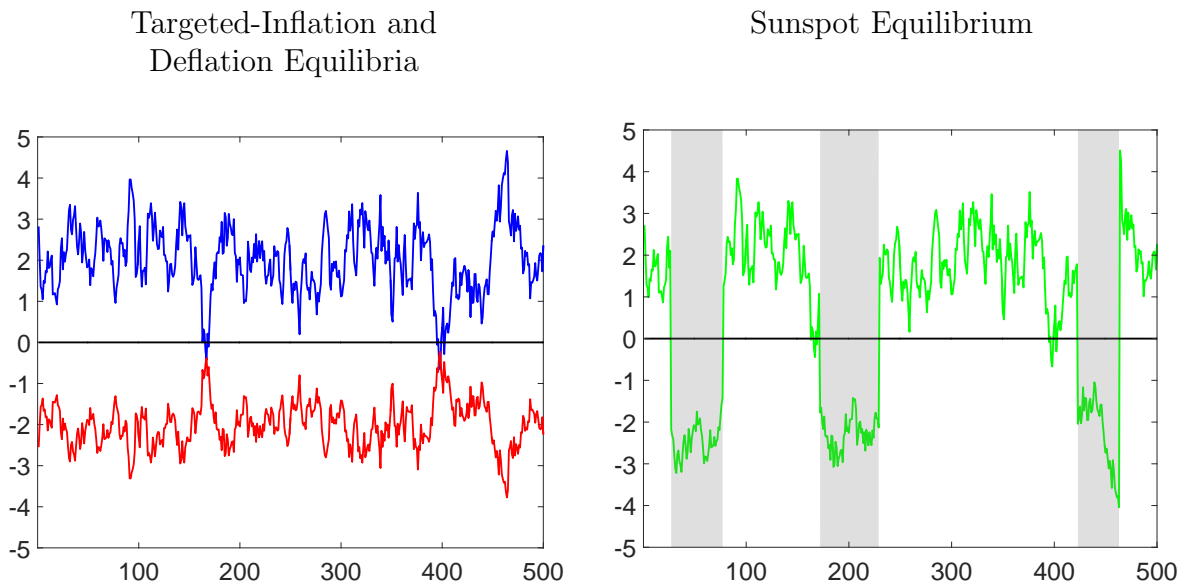
Because around the targeted-inflation steady state nominal interest rates respond to inflation

---

<sup>5</sup>It is assumed that the exogenous movements in  $\hat{M}_t$  are sufficiently small such that  $\psi\theta_1^*\hat{M}_t \leq \log(r\pi_*)$  for all  $t$ .



Figure 1: Inflation Dynamics in the Two-Equation Model



*Notes:* The figure shows annualized net inflation rate,  $400 \log \pi_t$ . In the left panel, the blue line shows the targeted-inflation equilibrium, and the red line shows the deflation equilibrium. In the right panel, the shaded area corresponds to periods in which the system is in the deflation regime,  $s_t = 0$ .

more than one-for-one, the local dynamics are unique.

We can also obtain a solution that fluctuates around the deflation steady state (henceforth deflation equilibrium):

$$\theta_0^D = -\log(r\pi_*), \quad \theta_1^D = -1. \quad (10)$$

Because around the deflation steady state nominal interest rates do not respond to inflation, the local dynamics are indeterminate and one could construct other solutions (see, for instance, Lubik and Schorfheide (2004) as well as the Online Appendix) that may involve a sunspot shock  $\zeta_t$  with the property that  $\mathbb{E}_{t-1}[\zeta_t] = 0$  or the dependence of inflation on  $\hat{M}_{t-1}$ . However, we will restrict our attention to (10). Note that (9) and (10) have drastically different dynamics: inflation and real interest rates have a positive correlation in the targeted-inflation equilibrium, while this correlation switches signs in the deflation equilibrium.

In the remainder of the paper we will focus on an equilibrium in which a two-state Markov-switching sunspot shock  $s_t \in \{0, 1\}$  triggers transitions from a targeted-inflation

Table 1: Decision Rule Coefficients

Targeted-Inflation Equilibrium	$\theta_0^* = 0$	$\theta_1^* = 1.5$
Deflation Equilibrium	$\theta_0^D = -0.01$	$\theta_1^D = -1$
Sunspot Equilibrium	$\theta_0(1) = -0.0002$ $\theta_0(0) = -0.0105$	$\theta_1(1) = 1.4611$ $\theta_1(0) = -1.1295$

regime to a deflation regime and vice versa:

$$\hat{\pi}_t^{(s)} = \theta_0(s_t) - \theta_1(s_t)\hat{M}_t \quad (11)$$

where  $\theta_0(s_t)$  and  $\theta_1(s_t)$  denote the regime-specific intercept and slope of the linear decision rule. Throughout the paper, we assume that the sunspot process  $s_t$  evolves independently from the fundamental shocks.<sup>6</sup> If the regimes are persistent, then the intercepts and slopes are similar in magnitude (but not identical) to the coefficients in (9) and (10), respectively. The precise values depend on the transition probabilities of the Markov switching process and ensure that (7) holds in every period  $t$ .

A numerical illustration is provided in Figure 1. We set  $\pi_* = 1.005$ ,  $\psi = 1.5$ ,  $r = 1.005$ ,  $\sigma = 0.0007$ ,  $\rho = 0.9$ ,  $p_{11} = 0.99$  and  $p_{00} = 0.95$ . The implied decision rule coefficients are summarized in Table 1. The left panel of Figure 1 compares the paths of annualized net inflation ( $400 \log \pi_t$ ) under the targeted-inflation equilibrium (9) and the deflation equilibrium (10). The inflation paths are shifted by the difference between  $400 \log \pi_*$  and  $400 \log(1/r)$ , which is 4%, and display perfect negative correlation. The right panel shows the sunspot equilibrium with visible shifts from the targeted-inflation regime to the deflation regime (shaded areas) and back.

---

<sup>6</sup>For simple models we were able to construct equilibria in which the Markov transition is triggered by  $\epsilon_t$ . But we were unable to numerically construct such solutions for the DSGE model presented in Section 3.

### 3 A Prototypical New Keynesian DSGE Model

Our quantitative analysis will be based on a small-scale New Keynesian DSGE model. Variants of this model have been widely studied in the literature and its properties are discussed in detail in Woodford (2003). The model economy consists of perfectly competitive final-goods-producing firms, a continuum of monopolistically competitive intermediate goods producers, a continuum of identical households, and a government that engages in monetary and fiscal policy. To keep the dimension of the state space manageable, we abstract from capital accumulation and wage rigidities. Unlike in Section 2, we will work directly with the nonlinear equilibrium conditions of this model. We will focus on a particular sunspot equilibrium that can capture transitions into and out of a regime in which interest rates are close to zero and inflation rates are low for an extended period of time. We describe the preferences and technologies of the agents in Section 3.1, and summarize the equilibrium conditions in Section 3.2.

#### 3.1 Preferences and Technologies

**Households.** Households derive utility from consumption  $C_t$  relative to an exogenous habit stock and disutility from hours worked  $H_t$ . We assume that the habit stock is given by the level of technology  $A_t$ , which ensures that the economy evolves along a balanced growth path. We also assume that the households value transaction services from real money balances, detrended by  $A_t$ , and include them in the utility function. The households maximize

$$\mathbb{E}_t \left[ \sum_{s=0}^{\infty} \beta^s d_{t+s} \left( \frac{(C_{t+s}/A_{t+s})^{1-\tau} - 1}{1-\tau} - \chi_H \frac{H_{t+s}^{1+1/\eta}}{1+1/\eta} + \chi_M V \left( \frac{M_{t+s}}{P_{t+s} A_{t+s}} \right) \right) \right], \quad (12)$$

subject to the budget constraint

$$P_t C_t + T_t + M_t + B_t = P_t W_t H_t + M_{t-1} + R_{t-1} B_{t-1} + P_t D_t + P_t S C_t.$$

Here  $\beta$  is the discount factor,  $d_t$  is a shock to the discount factor,  $1/\tau$  is the intertemporal elasticity of substitution,  $\eta$  is the Frisch labor supply elasticity, and  $P_t$  is the price of the final

good. The shock  $d_t$  captures frictions that affect intertemporal preferences in a reduced-form way. Fluctuations in  $d_t$  affect households patience and their desire to postpone consumption. As we demonstrate below, and as is commonly exploited in the literature, a sufficiently large shock to  $d_t$  makes the central bank cut interest rates all the way to the ZLB. The households supply labor services to the firms in a perfectly competitive labor market, taking the real wage  $W_t$  as given. At the end of period  $t$ , households hold money in the amount of  $M_t$ . They have access to a bond market where nominal government bonds  $B_t$  that pay gross interest  $R_t$  are traded. Furthermore, the households receive profits  $D_t$  from the firms and pay lump-sum taxes  $T_t$ .  $SC_t$  is the net cash inflow from trading a full set of state-contingent securities.

Detrended real money balances  $M_t/(P_t A_t)$  enter the utility function in an additively separable fashion. An empirical justification of this assumption is provided by Ireland (2004). As a consequence, the equilibrium has a block diagonal structure under the interest-rate feedback rule that we will specify below: the level of output, inflation, and interest rates can be determined independently of the money stock. We assume that the marginal utility  $V'(m)$  is decreasing in real money balances  $m$  and reaches zero for  $m = \bar{m}$ , which is the amount of money held in steady state by households if the net nominal interest rate is zero. Since the return on holding money is zero, it provides the rationale for the ZLB on nominal rates. More specifically since households can hold as well as issue debt at the market rate  $R_t$ , their problem does not have a solution when  $R_t < 1$ . The ZLB ensures the existence of a monetary equilibrium.

**Firms.** The final-goods producers aggregate intermediate goods, indexed by  $j \in [0, 1]$ , using the technology:

$$Y_t = \left( \int_0^1 Y_t(j)^{1-\nu} dj \right)^{\frac{1}{1-\nu}}.$$

The firms take input prices  $P_t(j)$  and output prices  $P_t$  as given. Profit maximization implies that the demand for inputs is given by

$$Y_t(j) = \left( \frac{P_t(j)}{P_t} \right)^{-1/\nu} Y_t.$$

Under the assumption of free entry into the final-goods market, profits are zero in equilibrium,

and the price of the aggregate good is given by

$$P_t = \left( \int_0^1 P_t(j)^{\frac{\nu-1}{\nu}} dj \right)^{\frac{\nu}{\nu-1}}. \quad (13)$$

We define inflation as  $\pi_t = P_t/P_{t-1}$ .

Intermediate good  $j$  is produced by a monopolist who has access to the following production technology:

$$Y_t(j) = A_t H_t(j), \quad (14)$$

where  $A_t$  is an exogenous productivity process that is common to all firms and  $H_t(j)$  is the firm-specific labor input. Intermediate-goods-producing firms face quadratic price adjustment costs of the form

$$AC_t(j) = \frac{\phi}{2} \left( \frac{P_t(j)}{P_{t-1}(j)} - \bar{\pi} \right)^2 Y_t(j),$$

where  $\phi$  governs the price stickiness in the economy and  $\bar{\pi}$  is a baseline rate of price change that does not require the payment of any adjustment costs. In our quantitative analysis, we set  $\bar{\pi} = \pi_*$ , where  $\pi_*$  is the target inflation rate of the central bank, which in turn is the steady state inflation rate in the targeted-inflation equilibrium. Firm  $j$  chooses its labor input  $H_t(j)$  and the price  $P_t(j)$  to maximize the present value of future profits

$$\mathbb{E}_t \left[ \sum_{s=0}^{\infty} \beta^s Q_{t+s|t} \left( \frac{P_{t+s}(j)}{P_{t+s}} Y_{t+s}(j) - W_{t+s} H_{t+s}(j) - AC_{t+s}(j) \right) \right]. \quad (15)$$

Here,  $Q_{t+s|t}$  is the time  $t$  value to the household of a unit of the consumption good in period  $t + s$ , which is treated as exogenous by the firm.

**Government Policies.** Monetary policy is described by an interest rate feedback rule. Because the ZLB constraint is an important part of our analysis we introduce it explicitly as follows:

$$R_t = \max \{1, R_t^* e^{\epsilon_{R,t}}\}. \quad (16)$$

Here  $R_t^*$  is the systematic part of monetary policy which reacts to the current state of the economy and  $\epsilon_{R,t}$  is a monetary policy shock. We consider two specifications for  $R_t^*$ , which

we refer to as *growth* and *gap* specifications. The growth specification takes the form

$$\text{Growth : } R_t^* = \left[ r\pi_* \left( \frac{\pi_t}{\pi_*} \right)^{\psi_1} \left( \frac{Y_t}{\gamma Y_{t-1}} \right)^{\psi_2} \right]^{1-\rho_R} R_{t-1}^{\rho_R}. \quad (17)$$

Here  $r$  is the steady-state real interest rate and  $\pi_*$  is the target-inflation rate. Provided that the ZLB is not binding, the central bank reacts to deviations of inflation from the target rate  $\pi_*$  and deviations of output growth from its long-run value  $\gamma$ .

Under the gap specification, the central bank reacts to a measure of the output gap in addition to inflation deviations from target:

$$\text{Gap : } R_t^* = \left[ r\pi_* \left( \frac{\pi_t}{\pi_*} \right)^{\psi_1} \left( \frac{Y_t}{Y_t^*} \right)^{\psi_2} \right]^{1-\rho_R} R_{t-1}^{\rho_R}, \quad (18)$$

where  $Y_t^*$  is the target level of output. In theoretical studies the targeted level of output often corresponds to the level of output in the absence of nominal rigidities and mark-up shocks, because from an optimal policy perspective, this is the level of output around which the central bank should stabilize fluctuations. However, historically, at least in the U.S., the central bank has tried to keep output close to the official measure of potential output, which is well approximated by a slow-moving trend. Thus we use exponential smoothing to construct  $Y_t^*$  directly from historical output data. It is given by

$$\log Y_t^* = \alpha \log Y_{t-1}^* + (1 - \alpha) \log Y_t + \alpha \log \gamma. \quad (19)$$

where  $\alpha$  is a parameter we calibrate such that  $\log Y_t^*$  tracks an official measure of potential output.

We use two alternative policy rules in an attempt to capture the dynamics of  $R_t^*$ , which is in principle latent when the economy is at the ZLB. For instance, the U.S. experienced a large negative rate of output growth in 2008:Q4. Under the growth rule, this creates a large drop in  $R_t^*$ , but the drop is short-lived because output growth subsequently recovers. Under the gap rule, the reduction in  $R_t^*$  is more persistent, because the level of output stays below its historical average for a long period of time. Our analysis is sensitive to the desired

interest rate, because  $R_t^*$  determines how constrained the central bank is by the ZLB and how likely it is that it will leave the ZLB in the subsequent quarters.

The government consumes a stochastic fraction of aggregate output. We assume that government spending evolves according to

$$G_t = \left(1 - \frac{1}{g_t}\right) Y_t. \quad (20)$$

The government levies a lump-sum tax  $T_t$  (or provides a subsidy if  $T_t$  is negative) to finance any shortfalls in government revenues (or to rebate any surplus). Its budget constraint is given by

$$P_t G_t + M_{t-1} + R_{t-1} B_{t-1} = T_t + M_t + B_t. \quad (21)$$

**Exogenous shocks.** The model economy is perturbed by four (fundamental) exogenous processes. Aggregate productivity evolves according to

$$\log A_t = \log \gamma + \log A_{t-1} + \log z_t, \text{ where } \log z_t = \rho_z \log z_{t-1} + \sigma_z \epsilon_{z,t}. \quad (22)$$

Thus, on average, the economy grows at the rate  $\gamma$ , and  $z_t$  generates exogenous stationary fluctuations of the technology growth rate around this long-run trend. We assume that the government spending shock follows the AR(1) law of motion

$$\log g_t = (1 - \rho_g) \log g_* + \rho_g \log g_{t-1} + \sigma_g \epsilon_{g,t}. \quad (23)$$

While we formally introduce the exogenous process  $g_t$  as a government spending shock, we interpret it more broadly as an exogenous demand shock that contributes to fluctuations in output. (20), (22) and (23) imply that log output and government spending are cointegrated and that the log government spending-output ratio is stationary. The shock to the discount factor evolves according to

$$\log d_t = \rho_d \log d_{t-1} + \sigma_d \epsilon_{d,t} \quad (24)$$

The monetary policy shock  $\epsilon_{R,t}$  is assumed to be serially uncorrelated. We stack the four innovations into the vector  $\epsilon_t = [\epsilon_{z,t}, \epsilon_{g,t}, \epsilon_{d,t}, \epsilon_{r,t}]'$  and assume that  $\epsilon_t \sim iidN(0, I)$ .

In addition to the fundamental shock processes, agents in the model economy observe an exogenous sunspot shock  $s_t$ , which follows a two-state Markov-switching process

$$\mathbb{P}\{s_t = 1\} = \begin{cases} (1 - p_{00}) & \text{if } s_{t-1} = 0 \\ p_{11} & \text{if } s_{t-1} = 1 \end{cases}. \quad (25)$$

### 3.2 Equilibrium Conditions

Because the exogenous productivity process has a stochastic trend, it is convenient to characterize the equilibrium conditions of the model economy in terms of detrended consumption  $c_t \equiv C_t/A_t$  and detrended output  $y_t \equiv Y_t/A_t$ . We write the consumption Euler equation (sometimes called the IS equation) as

$$c_t^{-\tau} = \beta R_t \mathcal{E}_t, \quad (26)$$

where

$$\mathcal{E}_t = \mathbb{E}_t \left[ \frac{d_{t+1}}{d_t} \frac{c_{t+1}^{-\tau}}{\gamma z_{t+1} \pi_{t+1}} \right]. \quad (27)$$

The solution algorithm approximates the conditional expectation  $\mathcal{E}_t$  using a Chebyshev polynomial in terms of the state variables. In a symmetric equilibrium, in which all firms set the same price  $P_t(j)$ , the price-setting decision of the firms leads to the condition

$$\begin{aligned} & \phi \beta \mathbb{E}_t \left[ \frac{d_{t+1}}{d_t} c_{t+1}^{-\tau} y_{t+1} (\pi_{t+1} - \bar{\pi}) \pi_{t+1} \right] \\ &= c_t^{-\tau} y_t \left\{ \frac{1}{\nu} \left( 1 - \chi_h c_t^\tau y_t^{1/\eta} \right) + \phi (\pi_t - \bar{\pi}) \left[ \left( 1 - \frac{1}{2\nu} \right) \pi_t + \frac{\bar{\pi}}{2\nu} \right] - 1 \right\}. \end{aligned} \quad (28)$$

A log-linearization of (28) leads to the standard New Keynesian Phillips curve.

We show in the Online Appendix that the aggregate resource constraint can be expressed as

$$c_t = \left[ \frac{1}{g_t} - \frac{\phi}{2} (\pi_t - \bar{\pi})^2 \right] y_t. \quad (29)$$

It reflects both government spending as well as the resource cost (in terms of output) caused



by price changes. Finally, we reproduce the monetary policy rule

$$\begin{aligned} \text{Growth: } R_t &= \max \left\{ 1, \left[ r\pi_* \left( \frac{\pi_t}{\pi_*} \right)^{\psi_1} \left( \frac{y_t}{y_{t-1}} z_t \right)^{\psi_2} \right]^{1-\rho_R} R_{t-1}^{\rho_R} e^{\sigma_R \epsilon_{R,t}} \right\}, \\ \text{Gap: } R_t &= \max \left\{ 1, \left[ r\pi_* \left( \frac{\pi_t}{\pi_*} \right)^{\psi_1} \left( \frac{y_t}{y_{t-1}^*} z_t \right)^{\alpha\psi_2} \right]^{1-\rho_R} R_{t-1}^{\rho_R} e^{\sigma_R \epsilon_{R,t}} \right\}. \end{aligned} \quad (30)$$

where  $y_t^* \equiv Y_t^*/A_t$ . We do not use a measure of money in our empirical analysis and therefore drop the equilibrium condition that determines money demand.

As the two-equation model in Section 2, the New Keynesian model with the ZLB constraint has two steady states, which we refer to as the targeted-inflation and the deflation steady states. In the targeted-inflation steady state, inflation equals  $\pi_*$  and the gross interest rate equals  $r\pi_*$ , while in the deflation steady state, inflation equals  $1/r$  and the interest rate is at the ZLB. Subsequently, we will focus on a stochastic sunspot equilibrium with a targeted-inflation regime ( $s_t = 1$ ) and a deflation regime ( $s_t = 0$ ).

## 4 Solution Algorithm

We now discuss some key features of the algorithm that is used to solve the nonlinear DSGE model presented in the previous section. Additional details can be found in the Online Appendix. We utilize a global approximation method following Judd (1992) where the decision rules are approximated by combinations of Chebyshev polynomials. The minimum set of state variables associated with our DSGE model is

$$\mathcal{S}_t = (R_{t-1}, y_{t-1}, d_t, g_t, z_t, \epsilon_{R,t}, s_t) \quad (31)$$

for the growth specifications and

$$\mathcal{S}_t = (R_{t-1}, y_{t-1}^*, d_t, g_t, z_t, \epsilon_{R,t}, s_t). \quad (32)$$

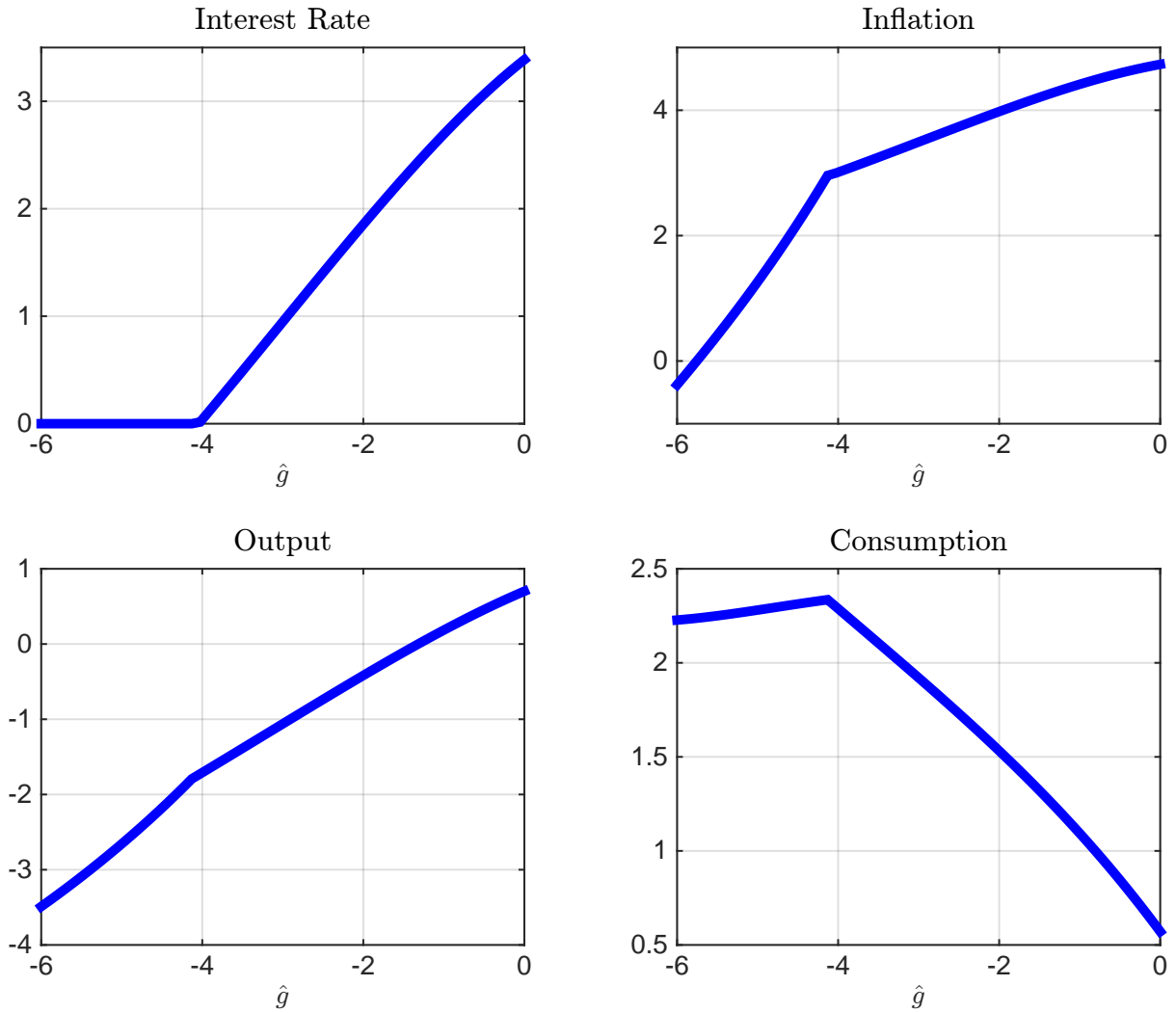
for gap specifications, and  $d_t$  is only relevant in the version with the discount factor shock. We included the regime-switching process  $s_t$  into the state vector because our goal is to characterize a sunspot equilibrium. An (approximate) solution of the DSGE model is a set of decision rules  $\pi_t = \pi(\mathcal{S}_t; \Theta)$ ,  $\mathcal{E}_t = \mathcal{E}(\mathcal{S}_t; \Theta)$ ,  $c_t = c(\mathcal{S}_t; \Theta)$ ,  $y_t = y(\mathcal{S}_t; \Theta)$ , and  $R_t = R(\mathcal{S}_t; \Theta)$  that solve the nonlinear rational expectations system given by (26) to (30), and the laws of motion of the exogenous processes. Note that conditional on  $\pi(\mathcal{S}_t; \Theta)$  and  $\mathcal{E}(\mathcal{S}_t; \Theta)$ , equations (26), (29) and (30) directly determine  $c(\mathcal{S}_t; \Theta)$ ,  $y(\mathcal{S}_t; \Theta)$ , and  $R(\mathcal{S}_t; \Theta)$ . Thus, we only use Chebyshev polynomials to approximate  $\pi(\mathcal{S}_t; \Theta)$  and  $\mathcal{E}(\mathcal{S}_t; \Theta)$ . In our notation the coefficient vector  $\Theta \equiv \{\theta_i\}$ ,  $i = 1, \dots, N$ , parameterizes all of the decision rules and  $N$  is the total number of coefficients.

The solution algorithm amounts to specifying a grid of points  $\mathcal{G} = \{\mathcal{S}_1, \dots, \mathcal{S}_M\}$  in the model's state space and determining  $\Theta$  by minimizing the (unweighted) sum of squared residuals associated with (27) and (28). Because (27) and (28) are functions of  $\mathcal{S}_t$ , we are evaluating the residuals for each  $\mathcal{S}_t \in \mathcal{G}$  and then sum the  $M$  squared residuals. There are two non-standard aspects of our solution method that we will now discuss in more detail: (i) the piecewise smooth representation of the functions  $\pi(\cdot; \Theta)$  and  $\mathcal{E}(\cdot; \Theta)$  and (ii) our iterative procedure of choosing grid points  $\mathcal{G}$ .

**Piece-wise Smooth Decision Rules.** The max operator in the monetary policy rule potentially introduces kinks in the decision rules  $\pi(\mathcal{S}_t)$  and  $\mathcal{E}(\mathcal{S}_t)$ . While Chebyshev polynomials, which are smooth functions of the states, can in principle approximate functions with a kink, such approximations are quite inaccurate for low-order polynomials. Thus, unlike Judd et al. (2010), Fernández-Villaverde et al. (2015), and Gust et al. (2012), we use a piece-wise smooth approximation of the functions  $\pi(\mathcal{S}_t)$  and  $\mathcal{E}(\mathcal{S}_t)$  by postulating

$$\pi(\mathcal{S}_t; \Theta) = \begin{cases} f_\pi^1(\mathcal{S}_t; \Theta) & \text{if } s_t = 1 \text{ and } R(\mathcal{S}_t) > 1 \\ f_\pi^2(\mathcal{S}_t; \Theta) & \text{if } s_t = 1 \text{ and } R(\mathcal{S}_t) = 1 \\ f_\pi^3(\mathcal{S}_t; \Theta) & \text{if } s_t = 0 \text{ and } R(\mathcal{S}_t) > 1 \\ f_\pi^4(\mathcal{S}_t; \Theta) & \text{if } s_t = 0 \text{ and } R(\mathcal{S}_t) = 1 \end{cases} \quad (33)$$

Figure 2: Sample Decision Rules



*Note:* This figure depicts the decision rules for 3vGrowth using parameter values estimated for the U.S. as described in Section 5.2. The x-axis corresponds to the state variable  $g_t$ , in percentage deviations from its steady state. The other state variables are fixed:  $s_t = 1$ ,  $R_{t-1} = 1$ , and  $y_{t-1}$ ,  $z_t$ , and  $\epsilon_{R,t}$  set to their means conditional on  $s_t = 1$ .

and similarly for  $\mathcal{E}(\mathcal{S}_t, \Theta)$ , where the functions  $f_j^i(\cdot)$  are linear combinations of a complete set of Chebyshev polynomials up to fourth order.

In our experience, the flexibility of the piece-wise smooth approximation yields more accurate decision rules, especially for inflation. Figure 2 shows a slice of the decision rules. We vary  $g_t$  over a wide range where the ZLB is both slack and binding. To generate the figure we condition on  $s_t = 1$ ,  $R_{t-1} = 1$  and set  $y_{t-1}$ ,  $z_t$ , and  $\epsilon_{R,t}$  to their means conditional

on  $s_t = 1$ . The monetary policy rule has a kink due to the ZLB, while the decision rule for inflation has an apparent kink due to the piece-wise smooth approximation in (33). The decision rules for output and consumption inherit the kinks in the decision rule for inflation (and  $\mathcal{E}(\mathcal{S}_t)$ ) and in the monetary policy rule. The kinks, especially the ones in the decision rules for inflation and consumption, are very severe. For instance, if the ZLB is binding, consumption is increasing in  $\hat{g}$ . If the ZLB is slack consumption falls as  $\hat{g}$  rises. As a consequence, a smooth approximation obtained from a single Chebyshev polynomial would do a very poor job capturing the actual decision rules.<sup>7</sup>

**Choice of Grid Points.** With regard to the choice of grid points, projection methods that require the solution to be accurate on a fixed grid, e.g., a tensor product grid, become exceedingly difficult to implement as the number of state variables increases above three. While the Smolyak grid proposed by Krueger and Kubler (2004) can alleviate the curse of dimensionality to some extent, we build on recent work by Judd et al. (2010), which proposed to simulate the model to be solved, to distinguish clusters on the simulated series, and to use the clusters' centers as a grid for projections.<sup>8</sup> We modify their methodology significantly by combining simulated grid points with states obtained from the data using a nonlinear filter. Doing so is necessary to capture the behavior of the model in low probability regions of the state space that are important for our analysis. For example, when  $s_t = 1$  ( $s_t = 0$ ), negative (positive) inflation is typically outside the ergodic distribution of the model.

**Determining the  $\Theta$  Coefficients.** We parameterize each  $f_j^i(\cdot)$  in (33) for  $i = 1, \dots, 4$  and  $j = \pi, \mathcal{E}$  with 210 parameters for a total of 1,680 elements in  $\Theta$ . We use  $M = 880$  gridpoints each, from the ergodic distribution and the filtered states, for a total of 1,760 residuals that come from the two equilibrium conditions. For a given set of filtered states and simulated grid points, the solution takes about six minutes on a single-core Windows-based computer using MATLAB where some computationally-intensive parts of the code are run using Fortran

---

<sup>7</sup>In an earlier version of the paper we indeed solved the model both ways and illustrated that the smooth approximation leads to approximation errors that are an order of magnitude larger relative to the piece-wise smooth approximation.

<sup>8</sup>The work by Judd, Maliar, and Maliar evolved considerably over time. We initially built on the working paper version, Judd et al. (2010). The published version of the paper, Maliar and Maliar (2015), also consider  $\epsilon$ -distinguishable (EDS) grids and locally-adaptive EDS grids. Their locally-adaptive grids are similar in spirit to our approach, which tries to control accuracy in a region of the state space that is important for the substantive analysis, even if it is far in the tails of the ergodic distribution.

via mex files. The approximation errors are in the order of  $10^{-4}$  on average, expressed in consumption units.

Because the set of simulated grid points that represent the ergodic distribution and the filtered states both depend on the solution of the model, some iteration of solution, on the one hand, and simulation and filtering, on the other hand, is required. For a given solution we simulate the model and get a set of points that characterize the ergodic distribution. We then run a particle filter, details of which are provided in the Online Appendix, to obtain the grid points which are consistent with data. We repeat this until we obtain a stable grid, which typically happens after three to five iterations.

## 5 Model Estimation and Dynamics

The data sets used in the empirical analysis are described in Section 5.1. In Section 5.2, we estimate the parameters of the DSGE model for the U.S. and Japan using data from before the economies reached the ZLB. These parameter estimates are the starting point for the subsequent analysis. We consider six different specifications for each country that differ in terms of the observable variables used and the details of the monetary policy rule. We solve the model using the nonlinear methods outlined in the previous section and in Section 5.3, we illustrate the dynamic properties of one of the estimated models by focusing on the economy's ergodic distributions and by presenting regime-specific impulse responses.

### 5.1 Data

The subsequent empirical analysis is based on log of real per-capita GDP, the log consumption-output ratio, GDP deflator inflation, and interest rates for the U.S. and Japan. The U.S. interest rate is the federal funds rate and for Japan we use the Bank of Japan's uncollateralized call rate. We consider two alternative consumption series. First, we use real personal consumption expenditures for the U.S. and real private consumption for Japan, where we normalize by an appropriate population measure to convert to per-capita terms. Doing this,

given the national income identity, combines investment, net exports and government spending into the latent variable  $G_t$ . As an alternative, we define consumption as all of output that is not government spending, which effectively makes  $G_t$  in the model track actual government spending in the data. Further details about the data are provided in the Online Appendix.

The time series are plotted in Figure 3. The U.S. sample starts in 1984:Q1, to coincide with the beginning of the Great Moderation, and ends in 2015:Q2. The time series for Japan range from 1981:Q1 to 2015:Q1. The vertical lines denote the end of the estimation sample for each country, 2007:Q4 for the U.S. and 1994:Q4 for Japan. We choose our estimation samples such that the observations pre-date the episodes of zero nominal interest rates and are consistent with the targeted-inflation regime. For the U.S. the fourth quarter of 2007 marks the beginning of the Great Recession, which was followed with a long-lasting spell of zero interest rate starting in 2009. The solid blue lines in the panels in the second row show the first measure of  $C/Y$  explained above, while the dashed green lines show the second measure.

In Japan, short-term interest rates dropped below 50 basis points in 1995:Q4 and have stayed at or near zero ever since. An important feature of the ZLB episode for Japan is consistently negative inflation rates – average inflation for Japan from 1999:Q1 to the end of the sample is nearly  $-1\%$ .<sup>9</sup> This is in stark contrast with the U.S., which experienced only two quarters of mildly negative inflation (2009:Q2 and Q3) and two quarters of inflation less than  $0.5\%$  at the very end of the sample. These features of the data are important (though not sufficient) for the identification of the sunspot regimes.

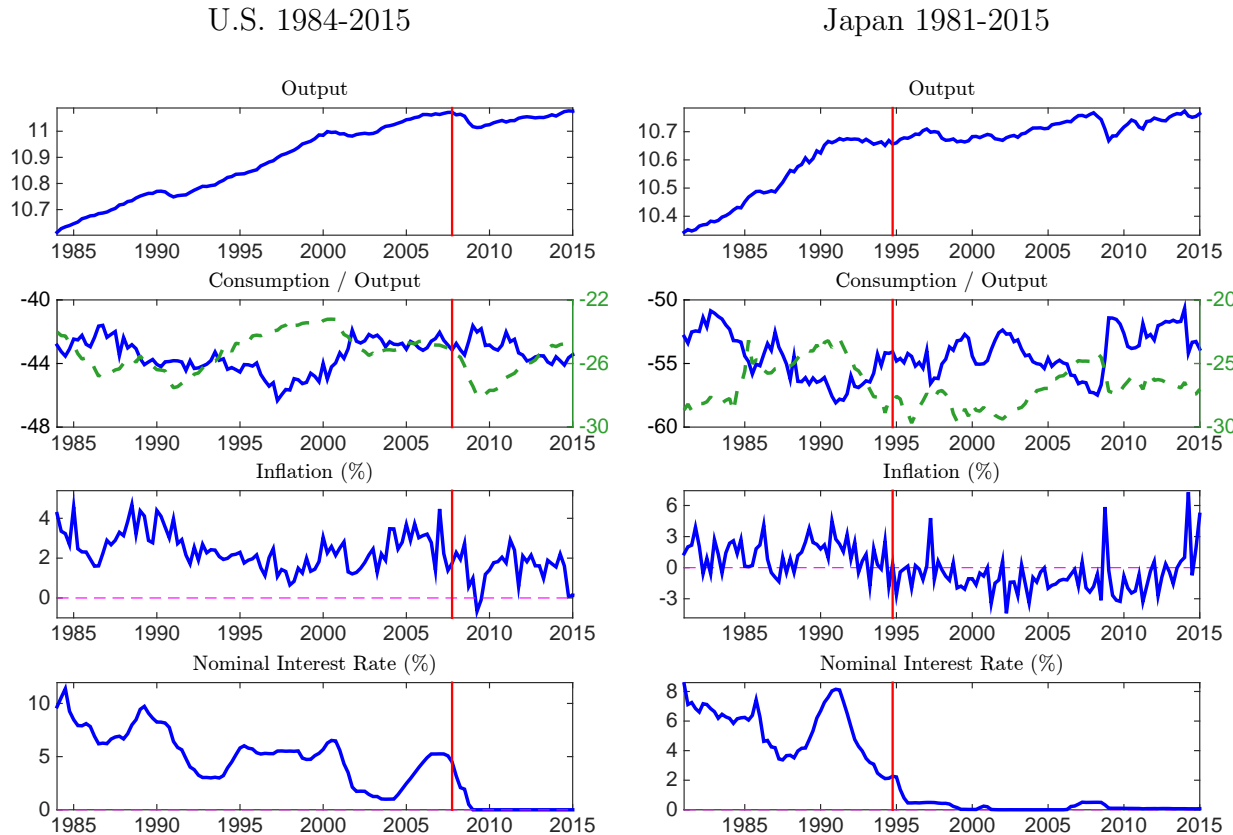
## 5.2 Model Estimation

For both the U.S. and Japan we estimate six versions of the DSGE model that differ in terms the monetary policy rules (growth vs. gap as in (30)) and the variables included

---

<sup>9</sup>The three positive spikes for Japanese GDP deflator inflation in 1997:Q2, 2008:Q4 and 2014:Q2 are unusual events that are not visible in, for instance, CPI inflation. The first and the third spike are due to increases in the value-added tax and the second is when a large decline in oil prices leads to a decrease in the import deflator which in turn generated a large jump in the GDP deflator. In our subsequent analysis we treat these observations as missing observations.

Figure 3: Data



*Note:* Output is the natural logarithm of per-capita output, consumption-output ratio is also in natural logarithm, scaled by 100, and inflation and nominal interest rate are in annualized percentage units. The blue lines in the panels in the second row plot private consumption to output ratio while the green lines plot the ratio of implied consumption to output where consumption is defined as all of output that is not government spending. The vertical red line in each figure show the end of the estimation sample.

in the estimation. For both countries, the first data set (three variables, henceforth 3v) comprises the log of output, inflation, and interest rates. The second data set (four variables, henceforth 4v) also includes the log consumption-output ratio. We use -C to denote the data set that uses private consumption as an observable and -G to denote the data set that makes government spending observable.

For the U.S. the 3v data set is the standard data set for the estimation of small-scale DSGE models in the literature before the Great Recession, with the minor difference that we use the level of output instead of output growth. In this version we treat consumption as a latent variable and switch off the discount factor shock. Thus, the model is driven by technology growth, government spending (aggregate demand) and monetary policy shocks,

which, again, is the typical specification for these models before the Great Recession. To estimate the DSGE model on the 4v data sets, we activate the discount factor shock, which is widely used in the ZLB literature to drive model economies to the ZLB. Using a variant of consumption as an observable is natural, because the discount rate shock influences consumption directly.

Recall that we choose the estimation samples such that the data favors the targeted-inflation regime. We verify that the values of the state variables that are needed to rationalize the observations fall into a region of the state space in which the decision rules of the nonlinear model are well approximated by the decision rules obtained from a first-order perturbation solution of the DSGE model that ignores the ZLB. The first-order perturbation solution can be computed much faster and is numerically more stable than the global approximation to the sunspot equilibrium discussed in Section 4. We use a standard random walk Metropolis-Hastings (RWMH) algorithm to estimate the log-linearized DSGE models over the pre-ZLB sample periods. The implementation of the posterior sampler follows An and Schorfheide (2007) and is described in the Online Appendix.<sup>10</sup>

We fix a subset of the parameters prior to the estimation. Several of these parameters can be calibrated without having to solve for the model dynamics. We choose values for  $\gamma$  and  $\beta$  such that the steady state of the model matches the average output growth, and interest rates over the estimation sample period.  $g_*$  is fixed to match the average consumption-output ratio in the data where consumption is based on the appropriate definition, with the 3v versions using the definition in 4v-C versions.

Because our sample does not include observations on labor market variables, we fix the Frisch labor supply elasticity. Based on Ríos-Rull et al. (2012), who provide a detailed discussion of parameter values that are appropriate for DSGE models of U.S. data, we set  $\eta = 0.72$  for the U.S. Our value for Japan is based on Kuroda and Yamamoto (2008) who use micro-level data to estimate labor supply elasticities along the intensive and extensive margin for males and females. The authors report a range of values which we aggregate into  $\eta = 0.85$ .

---

<sup>10</sup>The only somewhat nonstandard aspect of our methodology is the initialization of the Kalman filter to handle the nonstationarity in the log level of output.



The parameter  $\nu$ , which captures the elasticity of substitution between intermediate goods, is set to 0.1. It is not separately identifiable from the price adjustment cost parameter  $\phi$ . Finally, we calibrate the smoothing parameter  $\alpha$  for trend output in (19) to make the implied trend output close to a measure from the data. For the U.S. we use the output gap measure produced by the Congressional Budget Office, and for Japan we use the potential growth rate from the Bank of Japan to construct an output gap measure.

This leaves three parameters that cannot be estimated only based on pre-ZLB data: the central bank's target inflation rate  $\pi_*$ , and the transition probabilities of the sunspot process,  $p_{11}$  and  $p_{00}$ . Conditional on the transition probabilities, we adjust  $\pi_*$  such that average inflation conditional on  $s_t = 1$  roughly equals average inflation in the estimation sample. The  $\pi_*$  values we use for each specification / country are tabulated in the Online Appendix and we will now focus on the choice of the transition probabilities.

To avoid a computationally-costly calibration step that involves repeatedly solving for and simulating the sunspot equilibrium, we proceed as follows. We choose  $p_{11} = 0.99$  for both countries, reflecting our prior about the high persistence of the targeted-inflation regime. By choosing a value of  $p_{00}$  that is smaller than  $p_{11}$  we can ensure that the long-run inflation expectations stay on average positive in the deflation regime. We observe positive inflation expectations in both the U.S. and Japan. We set  $p_{00} = 0.95$  for the U.S. and equal to 0.92 for Japan. The unconditional probability of being in the deflation regime ( $s_t = 0$ ) is 0.17 for the U.S. and 0.11 for Japan.

Choosing a lower value for  $p_{00}$  for Japan than for the U.S. sets a higher threshold for concluding that the extended ZLB episode in Japan was associated with  $s_t = 0$ . Thus, this choice slightly biases our analysis against the widespread view that Japan has been trapped in a deflation regime. A lower bound for our choice of  $p_{00}$  is provided by the observation that the sunspot equilibrium ceases to exist if the deflation regime is too short-lived. This is discussed in Mertens and Ravn (2014) and confirmed in some numerical experiments in which we found the threshold to be around 0.90. The choice of transition probabilities affects the dynamics of long-run inflation expectations. Thus, we conduct a robustness exercise in Section 6.3, in which we show that our empirical results are not affected by the inclusion of

long-horizon inflation expectations data and that the model tracks these data with reasonable success. This, perhaps in an indirect way, validates our choices of transition probabilities.

For each country we estimate six DSGE model specifications: 3vGrowth, 4vGrowth-C, 4vGrowth-G, 3vGap, 4vGap-C and 4vGap-G. The marginal prior distributions for  $\tau$ ,  $\kappa$ ,  $\psi_1$ ,  $\psi_2$  and the parameters of the exogenous shock processes are tabulated in the Online Appendix. For the inverse IES  $\tau$  we use Gamma distributions with mean 2 and standard deviations of 0.25 (U.S.) and 0.5 (Japan). We re-parametrize the price adjustment cost parameter  $\phi$  in terms of the implied slope of the linearized New Keynesian Phillips curve:  $\kappa = \tau(1 - \nu)/(\nu\pi_*^2\phi)$ . Our prior for  $\kappa$  has a mean of 0.3 and a standard deviation of 0.1, encompassing fairly flat and fairly steep Phillips curves. Our benchmark priors for the policy rule coefficients  $\psi_1$  and  $\psi_2$  are centered at 1.5 and 0.5, respectively, with standard deviations of 0.3 and 0.25, respectively. For the 3-variable specifications, the likelihood function was fairly uninformative about the policy rule coefficients.<sup>11</sup> Thus, we replaced the benchmark prior distributions for  $\psi_1$  and  $\psi_2$  with tighter prior distributions. For the 3vGap specifications the modified priors are centered at the parameter values obtained from the estimation of the corresponding 4-variable specification with private consumption observable.

We truncate the prior distribution at the boundary of the determinacy region associated with the linearized version of the DSGE model. Thus, we are essentially imposing the existence of a second steady state (which requires that  $\psi_1 > 1$ ) when we are estimating the model. In view of the empirical results in Lubik and Schorfheide (2004) who estimate a similar model without imposing determinacy on post-1982 data and find no evidence in favor of  $\psi_1 < 1$ , the  $\psi_1 > 1$  restriction strikes us as reasonable.

The resulting posterior estimates reported in the Online Appendix are in line with the estimates reported elsewhere in the literature. Most notable are the implicit estimates of the slope of the New Keynesian Phillips curve, which range from 0.21 to 0.32 for the U.S. and 0.33 to 0.55 for Japan, implying fairly flexible prices and relatively small real effects of unanticipated interest rate changes.<sup>12</sup> The posterior distributions for most of the estimated

---

<sup>11</sup>This problem is well recognized in the literature; see, for instance, Cochrane (2011) for a theoretical appraisal and Mavroeidis (2010) for identification-robust inference in single-equation estimation settings.

<sup>12</sup>A survey of DSGE-model-based New Keynesian Phillips curve is provided in Schorfheide (2008). Our estimates fall within the range of the estimates obtained in the literature.

parameters move somewhat significantly away from their priors, or at least they get much tighter. A notable exception is the elasticity of intertemporal substitution parameter  $\tau$  for the U.S., which remains near the prior mean of 2.

### 5.3 Equilibrium Dynamics

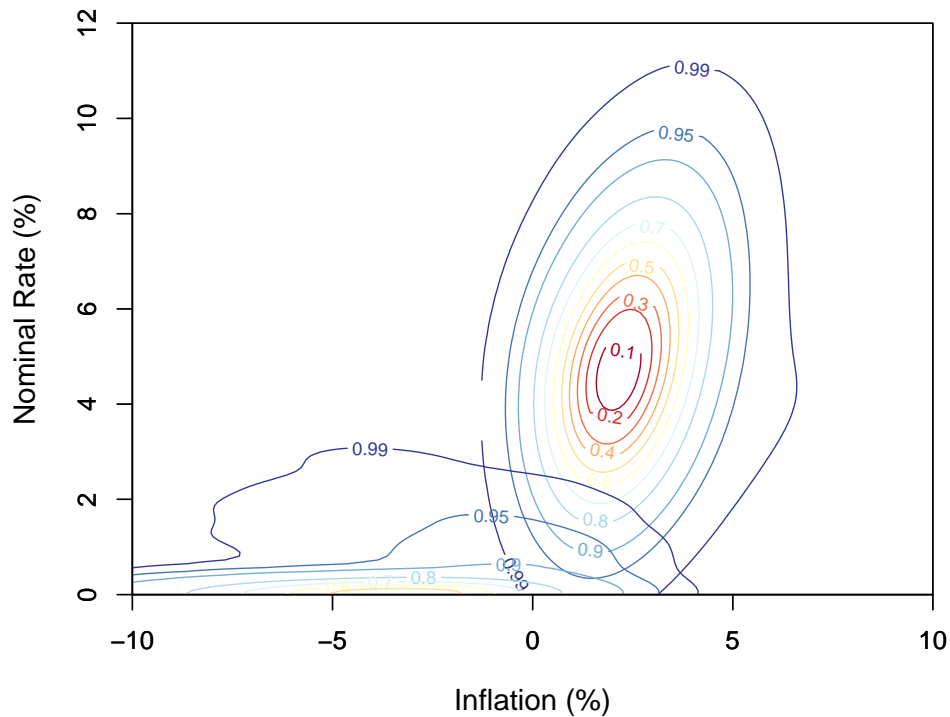
In this section we discuss the dynamics of the estimated specifications. It is impractical to report results for all 12 estimated specifications. Instead we focus on the 4vGrowth-C specification for the U.S. The other models behave qualitatively similarly, though sometimes there are quantitative differences, which we point out when relevant. We start with an illustration of the ergodic distribution by simulating a long sequence of observations. Figure 4 depicts contour plots for the joint probability density function of inflation and interest rates conditional on the regimes  $s_t = 0$  and  $s_t = 1$ , respectively. Formally, we show  $p(R_t, \pi_t | s_t = j)$  for  $j = 0, 1$ , which means that the two sets of contours are not weighted by the unconditional probabilities  $\mathbb{P}\{s_t = j\}$ . In the contour plots each line represents one percentile with the outermost line showing the 99<sup>th</sup> percentile. Under the deflation regime there is a high probability that the interest rate is equal to zero, which leads to a point mass on the  $x$ -axis and is not reflected in the contour plot.

As expected, the two regime-conditional distributions are approximately centered near the respective steady state values. Average inflation when  $s_t = 1$  is slightly above  $\pi_*$  (2.5% versus 2.4%) and average inflation conditional on  $s_t = 0$  is below inflation at the deflation steady state (−4.2% versus −2.8%). Under the targeted-inflation regime, inflation is positive with probability 99.7%. The probability of reaching the ZLB given  $s_t = 1$  is virtually zero given the shock processes estimated based on the pre-Great-Recession sample. This means that rationalizing the post-2008 U.S. experience with the targeted-inflation regime requires large shocks that are unlikely in view of the pre-2008 data. Under the deflation regime, on the other hand, interest rates are zero with 89% probability – even in the absence of extreme shocks – and inflation rates are negative with 97.6% probability.<sup>13</sup>

---

<sup>13</sup>Because average inflation in the estimation sample and hence  $\pi_*$  is lower in Japan, it is more likely to observe deflation when  $s_t = 1$  but virtually impossible to observe positive inflation when  $s_t = 0$ .

Figure 4: Regime-Conditional Ergodic Distribution: U.S. 4vGrowth-C

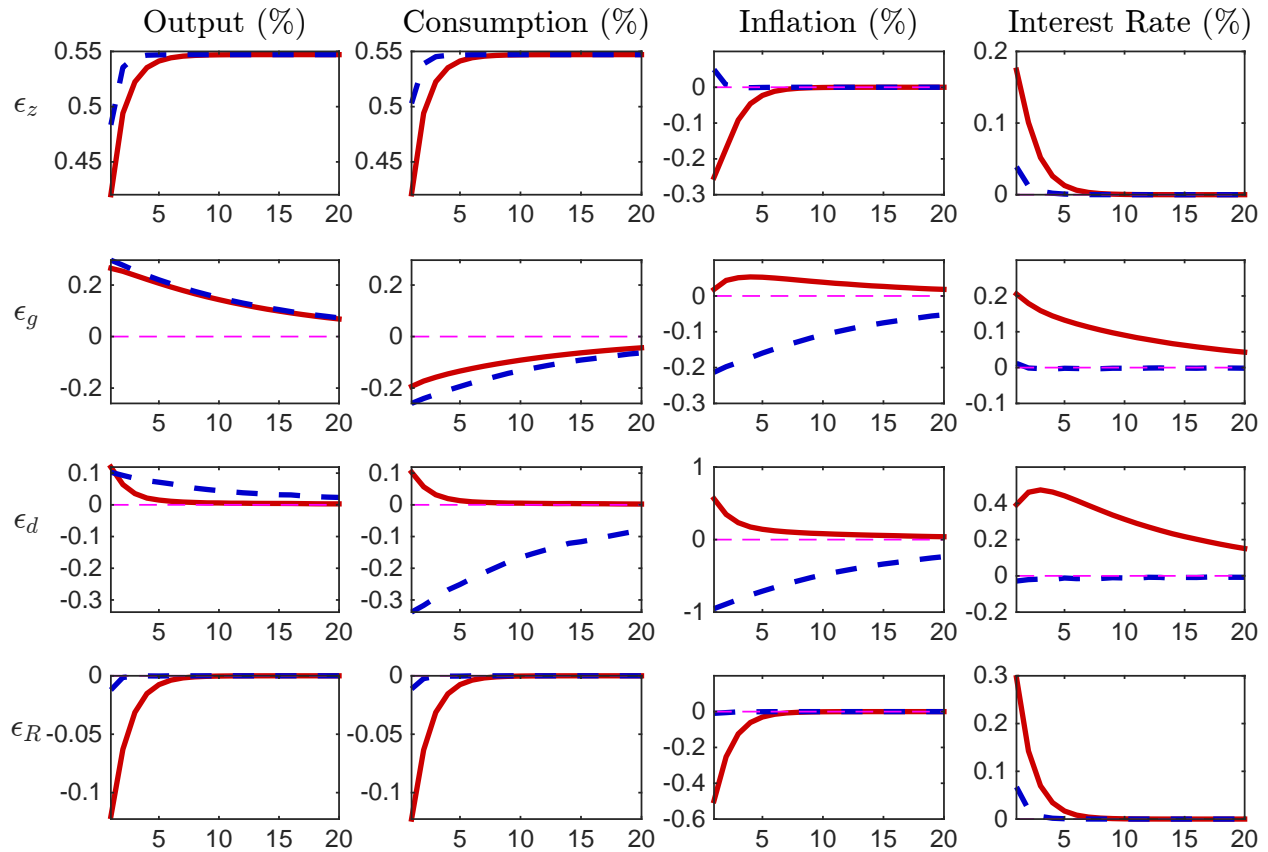


*Notes:* Figure depicts the joint probability density function (kernel density estimate) of annualized net inflation and interest rates conditional on the targeted-inflation regime and the deflation regime, respectively. Formally, the two sets of contours correspond to  $p(R_t, \pi_t | s_t = j)$  for  $j = 0, 1$ .

To better understand how the economy evolves in each regime, we compute impulse response functions (IRFs) to one standard deviation shocks conditional on remaining in the same regime throughout the response. Prior to the shock the economy is assumed to be at the mean of the regime-conditional ergodic distribution. The IRFs are plotted in Figure 5. Each column corresponds to one of the variables of interest (output, consumption, inflation, and interest rate) and each row corresponds to one of the structural innovations ( $\epsilon_{z,t}$ ,  $\epsilon_{g,t}$ ,  $\epsilon_{d,t}$ , and  $\epsilon_{R,t}$ ).

The responses conditional on  $s_t = 1$  are standard. The shock to technology raises output and consumption permanently. Because it is a supply shock, prices and quantities move in opposite directions. The reaction to the positive output growth dominates in the monetary policy rule and therefore the interest rate rises. The government spending shock acts like an aggregate demand shock, increasing output and inflation temporarily. In response the

Figure 5: Impulse Response Functions: U.S. 4vGrowth-C



*Notes:* The figure depicts impulse response functions to one-standard deviation shocks. The economy is assumed to be at the mean of the regime-conditional distribution when the shocks hit and to stay in the regime in the remaining periods. Solid lines depict the responses for  $s_t = 1$  and dashed lines show the responses for  $s_t = 0$ . For output and consumption the figure shows percentage deviations from the baseline path. For the interest rate and inflation it shows differences in annualized percentages relative to the baseline path.

central bank raises interest rates. Because nominal interest rates rise more strongly than inflation, the real interest rate increases, which reduces consumption.

To understand the response to the discount factor shock innovation  $\epsilon_{d,t}$ , recall that the stochastic discount factor  $M_{t+1}$  is a function of  $\beta d_{t+1}/d_t$ . In log-linear terms, an unanticipated rise in  $\hat{d}_t$  implies that  $\mathbb{E}_t[\hat{d}_{t+1} - \hat{d}_t] = (\rho_d - 1)\hat{d}_t$  is negative, because  $\hat{d}_t$  follows an AR(1) process. Thus, a positive  $\hat{d}_t$  shock makes the households less patient. This induces an increase in consumption and output, and an associated rise in inflation. The central bank reacts to these by increasing the interest rate, dampening the effect of the discount factor

shock. The discount factor can be interpreted as an aggregate demand shock in the sense that it generates positive comovement between output and inflation. Unlike an expansionary  $g_t$  shock, however, the  $d_t$  shock raises consumption.

A shock to monetary policy that increases the interest rate has the usual effects: output and inflation fall and, because the real interest rate rises, consumption falls as well. According to our estimates, the degree of price stickiness is relatively small and therefore the New Keynesian Phillips curve is relatively steep. Thus, the real effect of an unanticipated monetary policy shock is small (output and consumption drop by about 10 basis points) in comparison to the inflation response (annualized inflation falls by about 40 basis points).

The IRFs conditional on the  $s_t = 0$  regime display some important differences. In this case, a positive technology shock increases inflation slightly. On the other hand, positive government spending and discount factor shocks reduce inflation. Thus, the signs of the inflation responses switch, compared to the  $s_t = 1$  regime. This result is linked to the findings of Eggertsson (2011) and Mertens and Ravn (2014), who show that positive demand shocks may lead to a negative comovement of prices and output in the deflation regime.<sup>14</sup> The sign switching for the inflation response to the discount factor shock is the same phenomenon that we demonstrated in Section 2 for the simple model, in which inflation responds positively to a real-rate shock in the  $s_t = 1$  regime but negatively in the  $s_t = 0$  regime. We also observe in Figure 5 that consumption falls instead of rises in response to a discount factor shock because of the decline in the real interest rate. Finally, monetary policy is much less effective in the deflation regime.

## 6 Evidence of a Sunspot Switch

We are now ready to address our main empirical question: did the U.S. and Japan experience a change in regimes due to a switch in the sunspot variable at or near the beginning of their

---

<sup>14</sup>More specifically, Mertens and Ravn (2014) show that the EE curve, which plots inflation versus output using the relationship in (26), has two segments, one downward sloping and one upward sloping. If the equilibrium is in the upward-sloping portion, then a positive demand shock may generate a decrease in inflation while increasing output.

ZLB episodes? We do this in multiple steps. First, we examine the evidence that individual pairs of inflation and interest rate observations provide about the prevailing sunspot regime in Section 6.1. Second, in Section 6.2 we apply a nonlinear filter to six empirical specifications for each country and track the sunspot regime over time. We also compute predictive log likelihood scores that capture the fit of each specification and allow us to weight the model specifications and the implied regime probabilities based on their predictive performance. In Section 6.3 we examine the robustness of our empirical results to the inclusion of inflation expectations data. Finally, in Section 6.4 we present filtered structural shock innovations and their implicit narrative for the ZLB episodes in the two countries.

## 6.1 Static Analysis: Evidence from Inflation and Interest Rate Observations

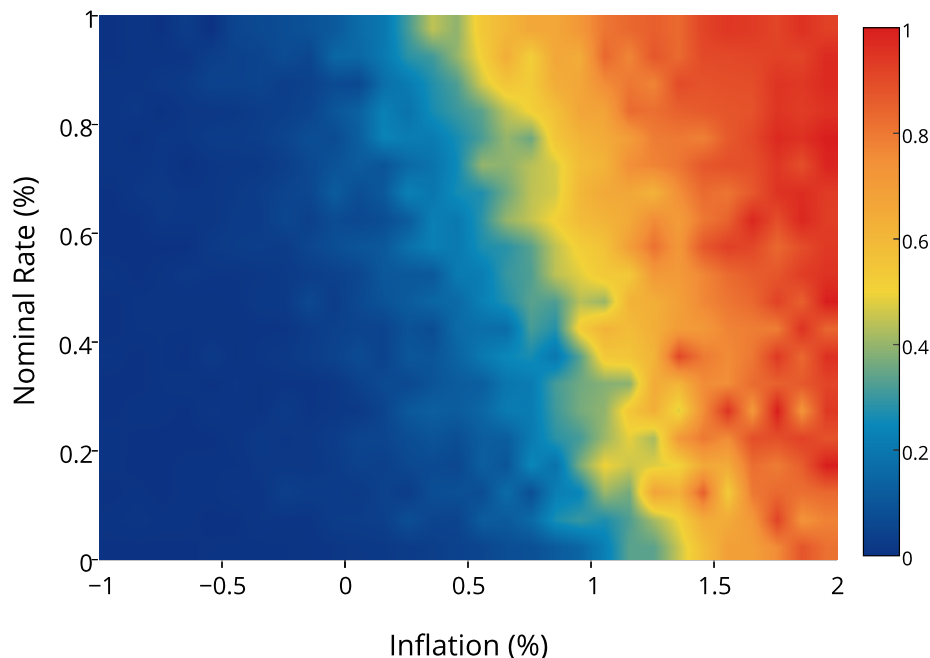
Our goal in this section is to conduct inference on the hidden process  $s_t$ . In Figure 4 we showed the bivariate ergodic distribution of  $(\pi_t, R_t)$  for the targeted-inflation and the deflation regimes. Glancing at Figure 4, it seems clear that an observation of a 3% inflation and a 6% interest rate is strong evidence in favor of  $s_t = 1$ . Conversely, zero interest rates combined with an inflation rate of -5% provides evidence for  $s_t = 0$ . However, if the interest rate is zero and inflation is low, as it has been the case for the U.S. since 2009, it is more difficult to determine by visual inspection which regime is favored by the data. The heatmap in Figure 6 (U.S. 4vGrowth-C) shows

$$\mathbb{P}\{s_t = 1 | R_t, \pi_t\} = \frac{p(R_t, \pi_t | s_t = 1) \mathbb{P}\{s_t = 1\}}{p(R_t, \pi_t | s_t = 1) \mathbb{P}\{s_t = 1\} + p(R_t, \pi_t | s_t = 0) \mathbb{P}\{s_t = 0\}} \quad (34)$$

for a section of the  $(\pi_t, R_t)$  space in which the evidence about the sunspot shock based on the contour plot in Figure 4 is ambiguous.<sup>15</sup> Suppose interest rates are around 25 basis points. Then an inflation rate of more than 1.5% would be interpreted as evidence for  $s_t = 1$  (indicated by the warm colors), whereas an inflation rate below 0.75% would be evidence in

---

<sup>15</sup>To generate the heatmap we define bins for inflation and interest rates and count the number of realizations within each bin based on a long simulation from the model. The probability that  $s_t = 1$  in a bin simply is the fraction of  $s = 1$  observations in that bin.

Figure 6:  $\mathbb{P}\{s_t = 1|\pi_t, R_t\}$ : U.S. 4vGrowth-C

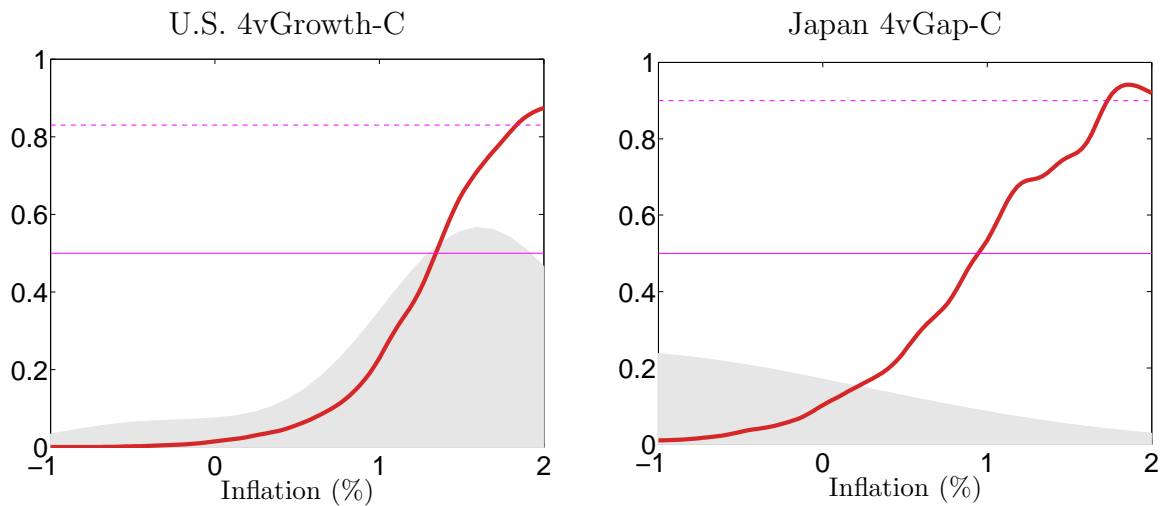
Notes: The legend for the colors is to the right of the heatmap.

favor of  $s_t = 0$  (indicated by dark blue).

Because our main interest is to infer the sunspot regime during the respective ZLB episodes of the U.S. and Japan, we want to zoom in to the bottom part of the heatmap figure. Thus, we now compute  $\mathbb{P}\{s_t = 1|ZLB, \pi_t\}$ , where we interpret interest rates in the range from 0% to 0.25% as the ZLB being binding. Results for 4vGrowth-C (U.S.) and 4vGap-C (Japan) are depicted in Figure 7. Unlike in the heatmap we now apply a kernel smoother to approximate the probabilities. We overlay kernel density estimates constructed from the observed inflation rates during the ZLB episodes.

Not surprisingly, the probabilities start at zero for low inflation observations and are increasing as inflation increases. The probabilities can be compared to three thresholds: 0.5,  $\mathbb{P}\{s_t = 1\}$ , and  $\mathbb{P}\{s_t = 1|ZLB\}$ . The first threshold is associated with a point estimator of  $s_t$  that is restricted to the set  $\{0, 1\}$ . As soon as the posterior probability of  $s_t$  exceeds 0.5, the point estimate (under a 0-1 loss function) is  $\hat{s}_t = 1$ . The second threshold is the prior probability of being in the targeted-inflation regime, which is 0.83 for the U.S.



Figure 7:  $\mathbb{P}\{s_t = 1|ZLB, \pi_t\}$ 

*Notes:* For the purposes of this figure ZLB is defined as interest rate being between 0% and 0.25%. The horizontal dashed line shows the country-specific threshold  $\mathbb{P}\{s_t = 1\}$ , which is 0.83 for the U.S. and 0.89 for Japan. The horizontal solid line is at 0.5. The shaded areas represent kernel density estimates constructed from the observed inflation rates during the ZLB episodes.

and 0.89 for Japan. If the inflation and interest rate pair exceeds the second threshold, then the data provide additional evidence in favor of the targeted-inflation regime. If the third threshold is exceeded, then the inflation observation increases the evidence against the deflation regime conditional on the economy being at the ZLB. The first two thresholds are shown by horizontal lines in Figure 7. The third threshold conditions on being at the ZLB. The probabilities  $\mathbb{P}\{s_t = 1|ZLB\}$  are close to zero for all specifications and are not shown.

As we saw in Figure 3, inflation rates in the U.S. were mostly positive and inflation rates in Japan were mostly negative during the ZLB period. For the U.S., using 0.5 as the cutoff for a point estimate of  $s_t$  that is restricted to zero or one, the 4vGrowth-C version implies that about half of the observations favor the targeted-inflation regime. However, relative to the prior distribution  $\mathbb{P}\{s_t = 1\}$ , the evidence in almost all of the inflation and interest rate observations leads to a downward revision of the probability that the economy is in the targeted-inflation regime. The negative inflation rates in combination with the 4vGap-C version for Japan provide strong evidence for a shift to the deflation regime. The probabilities  $\mathbb{P}\{s_t = 1|ZLB\}$  are below 0.5 for most of the inflation observations after 1999.

While individual inflation and interest rate observation provide some evidence about the regime, this evidence does not suffice to determine whether the U.S. or Japan did transition to the deflation regime. First, the economy evolves dynamically and the probability of being in one regime or another depends not only on the observed variables but also on the state of the economy, including the history of  $s_t$ . Second, variables other than inflation may contain key information that may help distinguish the two regimes – this is evident from Figure 6 by the wide yellow-colored region where the probability of being in the two regimes are about the same. In the next two sections we tackle these issues by using a nonlinear filter. While we focused on a single empirical model specification thus far, we will subsequently aggregate results from six specifications for each country based on their relative fit.

## 6.2 Dynamic Analysis: Evidence from a Nonlinear Filter

In this section we consider for both countries the six empirical specifications estimated in Section 5.2: 3vGrowth, 4vGrowth-C, 4vGrowth-G, 3vGap, 4vGap-C, and 4vGap-G. Each specification has a nonlinear state-space representation of the form

$$\begin{aligned} y_t^o &= \Psi(x_t) + \nu_t \\ x_t &= F_{s_t}(x_{t-1}, \epsilon_t) \\ \mathbb{P}\{s_t = 1\} &= \begin{cases} (1 - p_{00}) & \text{if } s_{t-1} = 0 \\ p_{11} & \text{if } s_{t-1} = 1 \end{cases} \end{aligned} \tag{35}$$

Here  $y_t^o$  is the vector of observables. We use the  $o$  superscript to distinguish the vector of observables from detrended output in our DSGE model. For the 3-variable specifications it consists of log of output, inflation, and nominal interest rates. For the 4-variable specifications the vector also includes the log consumption-output ratio.  $Y_{1:t}^o$  is the sequence  $\{y_1^o, \dots, y_t^o\}$ . The vector  $x_t$  stacks the continuous state variables, which are given by  $x_t = [R_t, y_t, y_t^*, y_{t-1}, d_t, z_t, g_t, A_t]'$ , and  $s_t \in \{0, 1\}$  is the Markov-switching process, where  $y_{t-1}$  is only necessary in the growth specifications,  $y_t^*$  is only necessary in the gap specifica-

tions, and  $d_t$  is only relevant for the 4-variable specifications.<sup>16</sup>

The first equation in (35) is the measurement equation, where  $\nu_t \sim N(0, \Sigma_\nu)$  is a vector of measurement errors. The second equation corresponds to the law of motion of the continuous state variables. The vector  $\epsilon_t \sim N(0, I)$  stacks the innovations  $\epsilon_{d,t}$ ,  $\epsilon_{z,t}$ ,  $\epsilon_{g,t}$ , and  $\epsilon_{R,t}$ , where once again  $\epsilon_{d,t}$  is used only in the 4-variable specifications. The functions  $F_0(\cdot)$  and  $F_1(\cdot)$  are generated by the model solution procedure described in Section 4. The third equation represents the law of motion of the Markov-switching process. Given the system in (35) and conditioning on the posterior mean estimates obtained in Section 5.2, we use a sequential Monte Carlo filter (also known as the particle filter) to extract estimates of the hidden sunspot shock process  $s_t$ , and the latent state  $x_t$ .<sup>17</sup>

**Model Weights.** While we will subsequently report estimates of the sunspot process  $s_t$  for each model specification, it is also important to have a method of weighing these specifications based on their goodness-of-fit and aggregating the empirical findings. The obvious difficulty here is that the four specifications do not share a common dataset. In order to compare 3-variable and 4-variable specifications, we follow the approach in Del Negro et al. (2016) and construct one-step-ahead predictive densities for the subset of common observations. Let  $z_t^o$  be the  $3 \times 1$  vector of output, inflation, and interest rates. These three variables are the core variables that most New-Keynesian models aim to capture. To weight the different models, we use the predictive density for  $z_t^o$  given specification  $\mathcal{M}_j$  and the  $t-1$  information set  $Y_{1:t-1}^o$ . This density is denoted by  $p(z_t^o | Y_{1:t-1}^o, \mathcal{M}_j)$  and can be aggregated into predictive log likelihoods (or predictive scores):<sup>18</sup>

$$\log \text{PS}_{T_0:T}(\mathcal{M}_j) = \sum_{t=T_0}^T \log p(z_t^o | Y_{1:t-1}^o, \mathcal{M}_j).$$

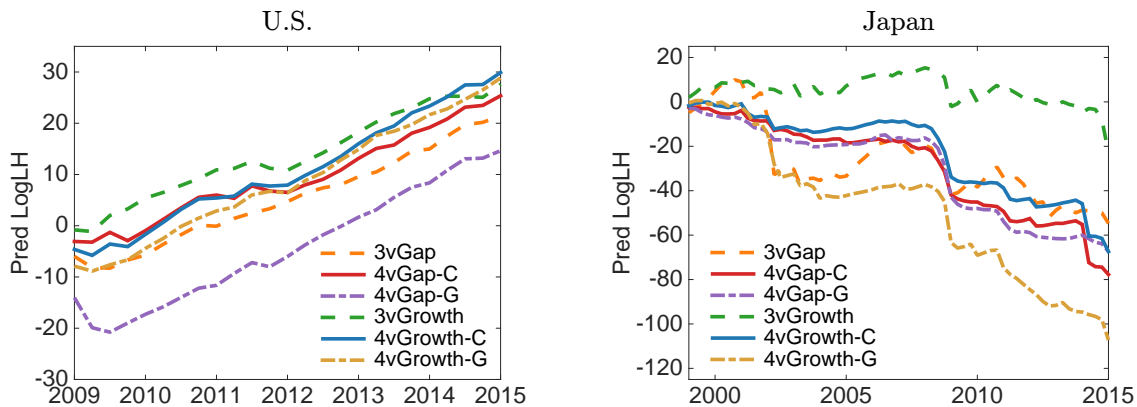
To compute the predictive score we condition on the posterior mean estimates obtained in

---

<sup>16</sup>The lower case output variables in the state vector are detrended by the level of technology  $A_t$ . The econometric state variables  $x_t$  of the state-space representation are slightly different from the economic state variables  $\mathcal{S}_t$  that appear in the solution.

<sup>17</sup>This filter is described in the Online Appendix. A more detailed exposition is provided in Herbst and Schorfheide (2015).

<sup>18</sup>The conditioning information set here differs across the 3-variable and 4-variable specifications. To avoid an overly tedious notation, we did not introduce a  $j$  index for the information set.

Figure 8: Cumulative Predictive Log Likelihood Scores  $\log \text{PS}_{T_0:T}(\mathcal{M}_j)$ 

Notes:  $T_0$  is the beginning of the ZLB episodes.

Section 5.2 and use the above-mentioned particle filter.

From an ex-ante perspective, the relative ranking of the 3- and 4-variable specifications based on the predictive density is undetermined. The 3-variable models are optimized to track the variables included in the  $z_t^o$  vector. The 4-variable models, on the one hand, have an additional degree of freedom, namely, the latent discount factor shock  $d_t$ , which can improve the tracking of the trivariate vector  $z_t^o$ . On the other hand, the 4-variable specifications also have to track the consumption-output ratio. Doing so may lead to a deterioration of the one-step-ahead forecast performance for  $z_t^o$ .

In Figure 8 we plot  $\log \text{PS}_{T_0:T}(\mathcal{M}_j)$  for each of the six model specifications for the U.S. and Japan. We take  $T_0$  to be the beginnings of the respective ZLB periods. For the U.S. the difference in fit between five of the six specifications is relatively small. The exception is the 4vGap-G version which performs consistently worse than the others. The performance differential between the best and the worst specification among these five specifications does not significantly widen over time, though the relative rankings do change. Until the end of 2013 the 3vGrowth specification dominates, whereas after 2014, the 4vGrowth-C specification attains the highest predictive score. For Japan the 3vGrowth specification also is best, though by a much larger margin. Unlike for the U.S., in the case of Japan the gap between the 3vGrowth specification and the five other specifications widens toward the end

of the sample.

Ex post, it turns out that one of the 3-variable specifications, namely 3vGrowth, dominates the 4-variable specifications. However, for both the U.S. and Japan, the 4-variable specifications are competitive with the 3vGap specification. Even though we are considering a period in which interest rates are zero, there seems to be information about the policy-rule specification (gap versus growth). This information arises from the fact that even if interest rates are currently zero, beliefs about the future conduct of monetary policy affect current output and inflation.

**Filtered Regime Probabilities.** Figure 9 depicts the filtered probabilities  $\mathbb{P}\{s_t = 1|Y_{1:t}^o\}$ , which can be thought of as a quasi-real-time assessment of the prevailing regime.<sup>19</sup> For each country we order the model specifications (from left to right, top to bottom) according to the predictive scores depicted in Figure 8.<sup>20</sup> As in Figure 7, we plot the prior  $\mathbb{P}\{s_t = 1\}$  as a dashed horizontal line in each panel. Using the simple rule by which  $\mathbb{P}\{s_t = 1|Y_{1:t}^o\} > 0.5$  is interpreted as evidence in favor of  $s_t = 1$ , we find that all but the 4vGap-C specification lead to the conclusion that the U.S. economy stayed in the targeted-inflation regime after 2008.

The strength of the evidence in favor of  $s_t = 1$  varies across specifications. Under the 3vGrowth specification the probability of  $s_t = 1$  dips shortly below 0.5 in 2009 and 2011 but quickly swings back to one. Conditional on the 4vGrowth-C specifications the probability of the targeted-inflation regime oscillates between 1.0 and 0.5. For 3vGap, 4vGap-G, and 4vGrowth-G the filtered probabilities are close to one. It is interesting to note that across the six specifications for the U.S. there is some uncertainty which vindicates Bullard (2010)'s concern of the possibility of a shift to the deflationary regime.

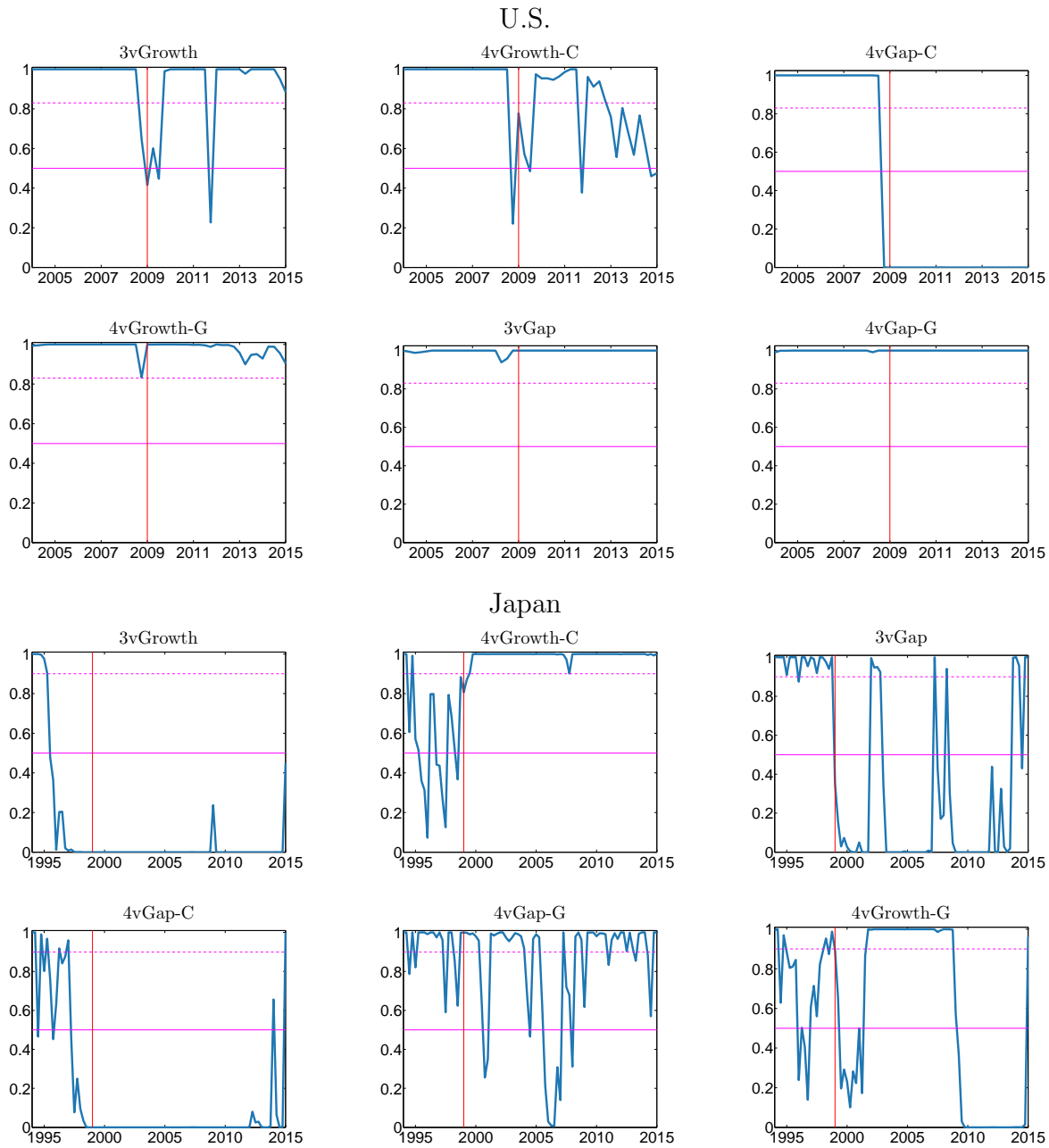
For Japan, we draw the opposite conclusions, though the results are less clear cut. The model with the highest predictive score, 3vGrowth, clearly implies a transition to the deflationary regime around 1997 and so does the 4vGap-C specification. According to 3vGap this transition occurred about two years later in 1999 and there have been a few instances in

---

<sup>19</sup>The qualifier “quasi” indicates that we are not using the actual real-time data vintages.

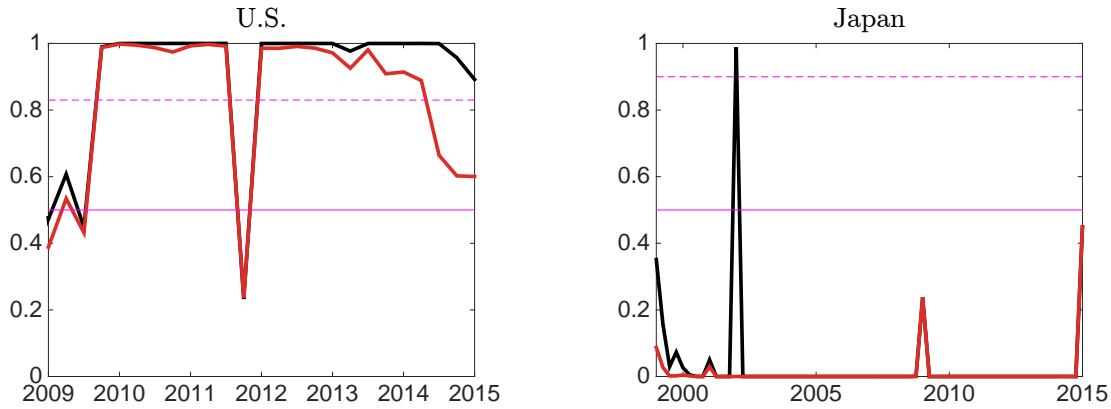
<sup>20</sup>For each period  $t$  we rank the models based on PS. We then compute the average rank to determine the order of the plots.

Figure 9: Filtered Probability of Targeted-Inflation Regime



*Notes:* The figure shows the filtered probabilities  $\mathbb{P}\{s_t = 1 | Y_{1:t}^o\}$  for each specification and country, starting five years prior to the start of the ZLB episode for the country. The dashed horizontal line shows the country-specific threshold  $\mathbb{P}\{s_t = 1\}$ , which is 0.83 for the U.S. and 0.89 for Japan. The solid horizontal line shows 0.5. The solid vertical line marks the beginning of the ZLB episode. The specifications are ordered according to fit.

which the Japanese economy seemed to escape the deflation regime for a short period. Ac-

Figure 10: Average  $\mathbb{P}\{s_t = 1|Y_{1:t}^o\}$  Across Specifications

*Notes:* We convert the cumulative log predictive score into quasi model probabilities (see (36)) and use them to compute a weighted average of  $\mathbb{P}\{s_t = 1|Y_{1:t}^o\}$  across the six specifications. We consider two choices of  $T_0$ : the beginning of the ZLB episodes (red) and the beginning of the estimation sample (black). The horizontal dashed line shows the country-specific threshold  $\mathbb{P}\{s_t = 1\}$ , which is 0.83 for the U.S. and 0.89 for Japan. The solid line indicates the 0.5 threshold.

cording to the 4v-G specifications the Japanese economy oscillated between the two regimes and the 4vGrowth-C specification implied that after an initial switch to the deflation regime around 1996 it reverted back to the targeted-inflation regime in 2000. On balance, we view these results as evidence for a switch to the deflation regime.

**Averaging the Regime Probabilities.** Based on the predictive densities, we can define the quasi model probabilities

$$\tilde{p}_t(\mathcal{M}_j) = \frac{\text{PS}_{T_0:T}(\mathcal{M}_j)}{\sum_{j=1}^4 \text{PS}_{T_0:T}(\mathcal{M}_j)} \quad (36)$$

and use them to weight the implications of different empirical specifications. Figure 10 shows the  $\tilde{p}_t(\mathcal{M}_j)$ -weighted regime probabilities computed for two choices of  $T_0$ : the beginning of the ZLB episodes (red) and the beginning of the estimation sample (black). The first choice is consistent with the predictive scores depicted in Figure 8. The second choice of  $T_0$  also factors in the fit of the model specifications prior to the ZLB episodes and thereby places more weight on the 3-variable specifications. After aggregating the information from the six specifications, we conclude that the U.S. has remained in the targeted-inflation regime in

the aftermath of the Great Recession and that Japan's ZLB experience is best described by a switch to the deflation regime.

For the U.S. there is significant uncertainty about the regime at the beginning of 2009. However, subsequently, there is only a single quarter, 2011:Q4, in which the probability of being in the targeted-inflation regime falls below 0.5. This quarter exhibits an unusually low inflation rate. In 2014, using the weights based on  $T_0=2009:Q1$  the probability of the targeted-inflation regime falls toward 0.5, because the 4vGrowth-C specification starts to dominate the weighted average. Recall from the bottom right panel of Figure 9 that the filtered probability of  $s_t = 1$  drops from 1 to about 0.5 between 2012 and the end of the sample. For Japan there is only one quarter in which the probability of being in the targeted-inflation regime clears all thresholds. This happens in 2002:Q1, when inflation is positive and seems like an outlier relative to the period before and after. Except in 2000 and in 2002:Q1 the black and the red lines are on top of each other, implying that the inference is not sensitive to the choice of  $T_0$ .

### 6.3 Incorporating Inflation Expectations

In our model, a regime shift triggered by the sunspot shock affects inflation expectations. In turn, movements in inflation expectations can be informative about the occurrence of a regime shift. As a robustness exercise we augment the measurement equations for the model with the highest predictive score (3vGrowth for both the U.S. and Japan) with a measurement equation for long-run inflation expectations.

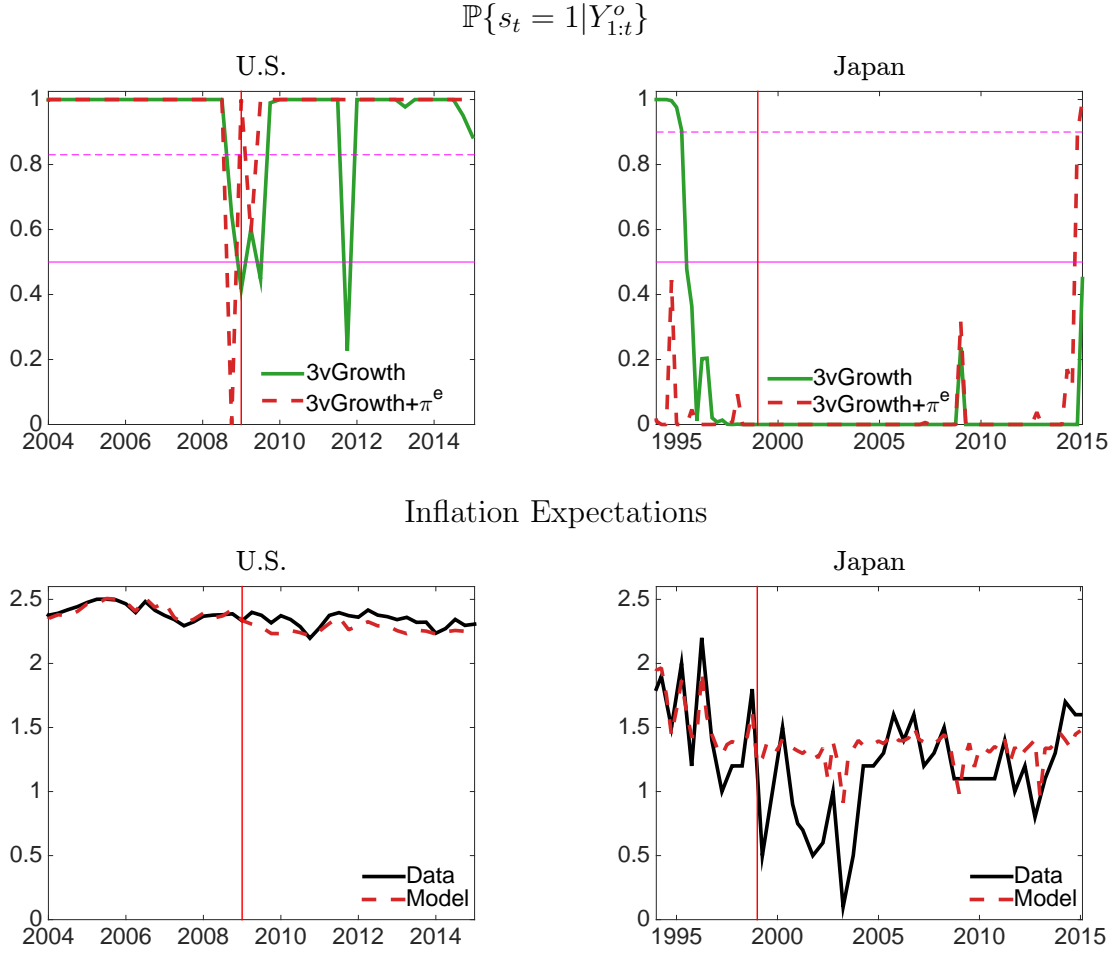
Defining inflation as the change in the natural logarithm of the price level, long-run inflation expectations are equal to the annualized average of expectations of quarterly inflation over an extended period of time. In the context of our model, we are interested in

$$\pi_t^e(\mathcal{S}_t) = \frac{1}{41 - h_0} \mathbb{E} \left[ \sum_{h=h_0}^{40} 400 \log [\pi(\mathcal{S}_{t+h})] \mid \mathcal{S}_t \right]. \quad (37)$$

The starting point  $h_0$  is determined by the horizon of long-run inflation expectations in the data. It will be set to 1 for the U.S. and 21 for Japan.  $\mathcal{S}_t$  is the vector of state variables defined



Figure 11: Incorporating Inflation Expectations



*Notes:* Top panels:  $\mathbb{P}\{s_t = 1 | Y_{1:t}^o\}$  for the 3vGrowth models for both countries. Green solid line is from the version that does not use inflation expectations in the filter. Red dashed line is the result of the filtering when inflation expectations is added to the list of observables in the filter. See the notes to Figure 9 for a description of the horizontal lines. Bottom panels: Inflation expectations as defined in the text, data and as obtained from the model.

in (31) and  $\pi(\mathcal{S}_t)$  is the agents' decision rule for inflation. We approximate this expectation via simulation. Given a value  $\mathcal{S}_i$  for the state, we simulate the economy over 40 periods for  $N$  different paths of the stochastic variables, including the sunspot variable, using the decision rules that we had previously computed.  $\hat{\pi}^e(\mathcal{S}_i)$  is a Monte Carlo approximation of (37) obtained by averaging the inflation trajectories over time horizon  $h$  and the  $N$  simulations. Because we need to use  $\pi^e(\cdot)$  in the particle filter as a function of  $\mathcal{S}_t$ , we use Chebyshev polynomials to obtain a piece-wise-smooth approximation of the function in-between the

grid points  $\mathcal{S}_i$  for which we have simulated the inflation expectations.

For the U.S. we use the 10-year ahead inflation expectations produced by Aruoba (2014). For Japan, we use the 6-to-10-year inflation expectations produced by Consensus Economics.<sup>21</sup> The *levels* of these forecasts do not directly match those that come from our model for the two countries. Because we are mostly interested in using the *changes* in the long-run expectations when the economies transition to the ZLB to inform the filter about changes in the sunspot variable, we adjust the inflation expectation data by adding the difference between the model-implied and the observed average inflation expectations during the estimation period.

Figure 11 shows the results of this robustness exercise. The top panel shows filtered probabilities  $\mathbb{P}\{s_t = 1|Y_{1:t}^o\}$  using inflation expectations as an additional observed variable, allowing for a measurement error. We deduce from the comparison with the baseline results (obtained without expectations data) that the main conclusion does not change. For the U.S., after some uncertainty about  $s_t$  during the turbulent period between 2008:Q3 and 2009:Q2,  $s_t$  is essentially zero from 2009:Q3 onwards. For Japan, the sunspot switch is likely to have occurred somewhat earlier and lasts until the last few periods of our sample.

The bottom panels of Figure 11 plot the inflation expectations data we use in the filtering process and the model-implied values. The discrepancy is attributed to measurement errors. The fit is quite remarkable: the correlations between the data and the model values are 0.77 for the U.S. and 0.72 for Japan. Most importantly, the model matches the near constancy of inflation expectations in the U.S. pre- and post-ZLB and, for the most part, the decline in Japan. Note that positive inflation expectations in Japan are not inconsistent with a switch to the deflation regime. Conditional on  $s_t = 0$  there is an 8% probability of a switch to  $s_{t+1} = 1$ , which leads to a substantial probability of a switch to the targeted-inflation regime sometime over the next 40 quarters. In turn, while actual inflation will be negative during the  $s_t = 0$  spell, long-run expectations need not be negative.

---

<sup>21</sup>The Japanese 6-to-10 year expectation data in Figure 11 appear to be excessively volatile. Two possible explanations are that (i) several of the survey respondents reported 10-year expectations; or (ii) the number of respondents is small, which introduces noise in the cross-sectional aggregate. Nonetheless, we link the Japanese data to 6-to-10-year model-implied inflation forecasts.

To sum up, using inflation expectations confirms the conclusion we reached in the previous sections – that the U.S. did not switch to a deflation regime, while Japan did – and our model is able to match the broad patterns in the inflation expectations data.

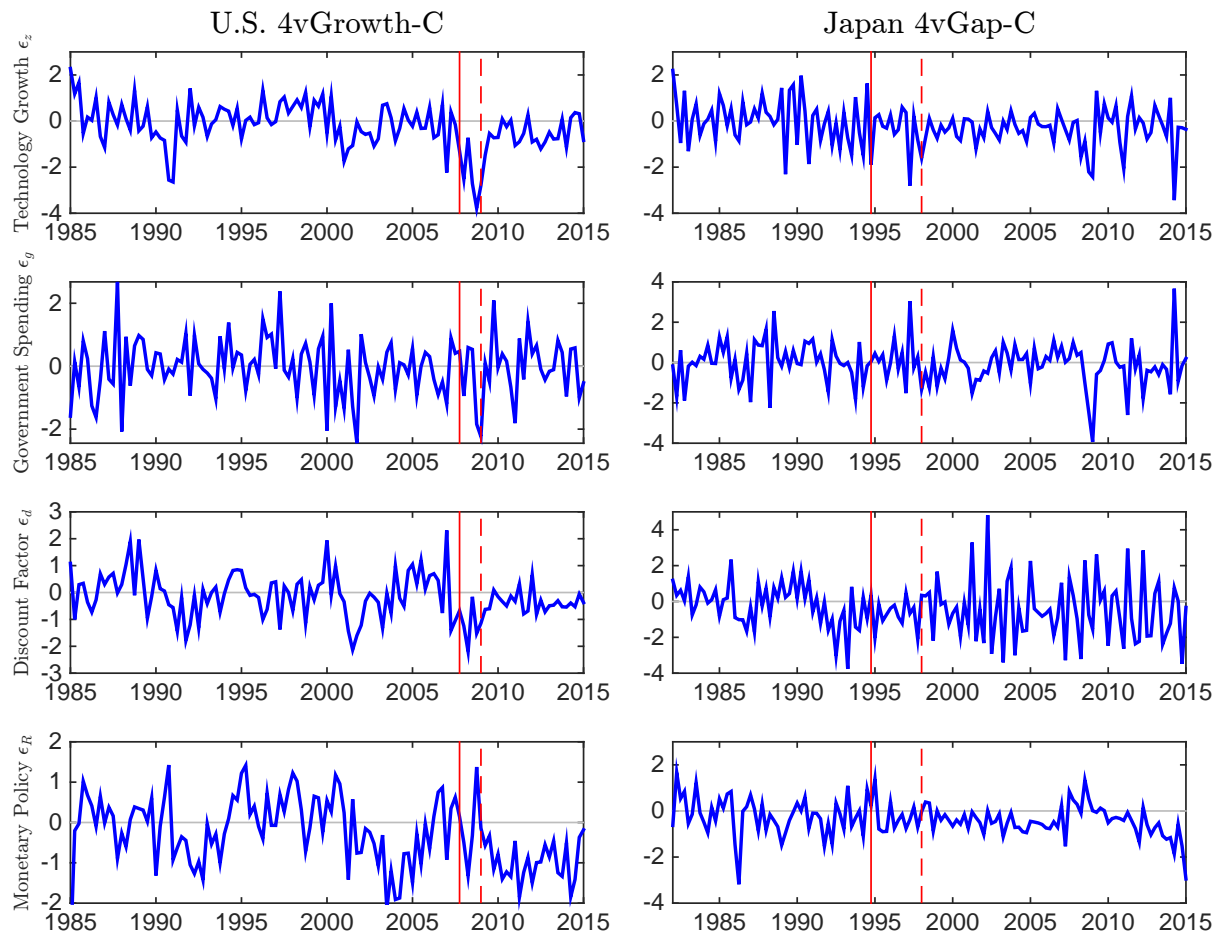
## 6.4 Filtered Shocks and Narrative

The filter also generates estimates of the exogenous shock processes and their innovations. The subsequent discussion focuses on the 4vGrowth-C specification for the U.S. and the 4vGap-C specification for Japan. The inference about  $s_t$  from these two specifications is by and large consistent with the conclusions drawn after aggregation across the six specifications for each country. Using these 4v versions allows us to extract the path for the discount factor shock, which is the typical shock the literature uses to trigger a ZLB episode. Time series plots for the filtered innovations  $\epsilon_t$  are provided in Figure 12. Recall that in these versions of our model  $\log C_t/Y_t \approx -\log g_t$  (in a first-order approximation of the aggregate resource constraint the relationship holds exactly). Thus, the government spending shock by construction tracks the log output-consumption ratio. In the last quarter of 2008, the U.S. experienced a large drop in output, which turned out to be permanent. In our model, this is captured by a negative technology growth shock of roughly 3.5 standard deviations. In addition, the aggregate demand shock  $g_t$  dropped by about 2 standard deviations and the discount factor innovation is also negative in 2008:Q4. All three adverse shocks generate a drop in interest rates (see Figure 5) and push the economy toward the ZLB. While the two adverse demand shocks are deflationary, the adverse technology shock is inflationary. This is consistent with the modest decline in inflation.<sup>22</sup>

After 2008:Q4, the technology growth shocks stay slightly negative on average, depressing output growth and preventing a quick and full recovery. The discount factor shock innovations also remain on average negative, delaying the mean reversion of the  $d_t$  process

---

<sup>22</sup>Due to the simplicity of the DSGE model, the shock decomposition is not refined enough to generate a more detailed narrative of the recent U.S. experience that emphasizes the disruption in financial intermediation. Shocks to the financial system and nonlinearities generated by its disruption, are interpreted as large technology or discount factor shocks by our model. There is, however, independent evidence of a decline in total factor productivity in this period. Christiano et al. (2015) document a sustained decline in various measures of neutral technology during this period, including Fernald's (2012) utilization-adjusted TFP measure.

Figure 12: Filtered Shock Innovations  $\epsilon_t$ 

*Note:* Innovations are shown in multiples of their standard deviations. The solid vertical line shows the end of the estimation sample and the dashed vertical line shows the beginning of the ZLB episode.

and keeping the economy near the ZLB. Moreover, the filtered sequence of monetary policy shocks is mostly negative. Our simulations show that in the absence of these shocks interest rates would have been between 0.75% and 1%. Thus, from the perspective of the DSGE model, U.S. monetary policy is more expansionary in the aftermath of the Great Recession than what is implied by the systematic part of the interest rate feedback rule.

Given the long-lasting drop in output, one might expect the Phillips curve relationship in the DSGE model to imply a significant deflation, which did not occur in the U.S.. In this regard, our simple DSGE models works similarly as the richer DSGE model studied in Del Negro et al. (2015). One important reason for why the New Keynesian Phillips curve

embedded in the DSGE model does not predict deflation is that the Phillips curve is forward looking. Inflation depends on the sum of discounted expected future marginal costs. Because the model has a fairly strong mean reversion, it predicts marginal costs to rise in the medium run, which allows the model to explain what the literature has termed the “missing deflation” in the U.S. Moreover, the expansionary monetary policy contributed to the positive inflation rates.

The 4vGap-C specification for Japan implies that the economy transitioned to the deflation regime in the late 1990s. In the deflation regime the negative inflation rates generate a non-negligible resource cost and the approximation  $\log C_t/Y_t \approx -\log g_t$  is no longer accurate. The discount factor shock also affects the consumption-output ratio. As is apparent from the impulse responses in Figure 5, none of the shocks has a significant impact on the interest rates, which are with high probability zero. The filter essentially inverts these relationships. Most notably, the slow growth of the Japanese economy since the late 1990s maps into technology growth innovations that are on average negative. An inspection of the regime-conditional ergodic distributions drawn in Figure 4 indicates that inflation rates in the deflation regime are with high probability less than -4%.<sup>23</sup> Actual Japanese inflation, while being negative, has always been above -4%, which is translated by the filter in a sequence of discount factor innovations that are fairly volatile and on average below zero.

## 7 Conclusion

The recent experiences of the U.S. and Japan have raised concern among policy makers about a long-lasting switch to a regime in which interest rates are zero, inflation is low, and conventional macroeconomic policies are less effective. We solve a small-scale New Keynesian DSGE model imposing the ZLB constraint and introducing a non-fundamental Markov sunspot shock that can move an economy between a targeted-inflation regime and a deflation regime. An economy may be pushed to the ZLB either by successive fundamental shocks (e.g., an adverse discount factor shock) in the targeted-inflation regime or by a switch

---

<sup>23</sup>The contours for 4vGap-Japan look similar to the contours for 4vGrowth-U.S., which are shown in the figure.

to the deflation regime. We develop a quantitative framework that can distinguish these two possibilities.

Our empirical analysis focuses on the U.S. and Japan and utilizes six different DSGE model specifications for each country that differ in terms of the observables used and the monetary policy rule. Using a nonlinear filter, we find that for the U.S. five of the six specifications essentially agree: the U.S. remained in the targeted-inflation regime during its ZLB episode, with the possible exception of the early part of 2009 where evidence is ambiguous. The evidence for Japan is less clear-cut. Four out of six model specifications imply that Japan spent a significant amount of time in the deflation regime since the late 1990s. After aggregating results across model specifications based on predictive scores for output, inflation, and interest rates, we conclude that the U.S. did not and Japan did transition to the deflation regime.

Our model is silent as to why the two experiences are different because the sunspot process in our model is purely exogenous. In a richer, but computationally much more challenging specification, the coordination of beliefs may be correlated with fundamentals and be affected by central bank actions. Perhaps one key difference between Japan in 1999 and the U.S. in 2009 is in their conduct of monetary policy. Ito and Mishkin (2006), who provide a summary of the actions taken by the Bank of Japan and the Japanese government conclude that “(...) mistakes in the management of expectations [by the Bank of Japan] are a key reason why Japan found itself in a deflation that it is finding very difficult to get out of”.<sup>24</sup> The actions of U.S. policymakers contrast greatly with those of the Bank of Japan. The Federal Reserve and in general policy makers in the U.S. enacted unconventional policies such as quantitative easing and forward guidance and evidently did a good job in coordinating inflation expectations near its target. We leave a formal quantitative analysis for future research.

---

<sup>24</sup>Ueda (2012) provides a very thorough review of the policies used in the U.S. and Japan and he concludes that “the Japanese economy seems to be trapped in an ‘equilibrium’ whereby only exogenous forces generate movements to a better equilibrium with a higher rate of inflation.”

## References

- AN, S. AND F. SCHORFHEIDE (2007): “Bayesian Analysis of DSGE Models,” *Econometric Reviews*, 26, 113–172.
- ARMENTER, R. (2014): “The Perils of Nominal Targets,” *Manuscript, Federal Reserve Bank of Philadelphia*.
- ARUOBA, S. B. (2014): “Term Structure of Inflation Expectations and Real Interest Rates: The Effects of Unconventional Monetary Policy,” *Manuscript, University of Maryland*.
- BENHABIB, J. AND R. E. FARMER (1999): “Indeterminacy and sunspots in macroeconomics,” in *Handbook of Macroeconomics*, ed. by J. B. Taylor and M. Woodford, Elsevier, vol. 1, Part A, 387 – 448.
- BENHABIB, J., S. SCHMITT-GROHÉ, AND M. URIBE (2001a): “Monetary Policy and Multiple Equilibria,” *The American Economic Review*, 91, 167–186.
- (2001b): “The Perils of Taylor Rules,” *Journal of Economic Theory*, 96, 40–69.
- BONEVA, L. M., R. A. BRAUN, AND Y. WAKI (2016): “Some unpleasant properties of loglinearized solutions when the nominal rate is zero,” *Journal of Monetary Economics*, 84, 216 – 232.
- BULLARD, J. (2010): “Seven Faces of ‘The Peril’,” *Federal Reserve Bank of St. Louis Review*, 92, 339–352.
- CASS, D. AND K. SHELL (1983): “Do Sunspots Matter?” *Journal of Political Economy*, 91, 193–227.
- CHRISTIANO, L. J., M. EICHENBAUM, AND M. TRABANDT (2015): “Understanding the Great Recession,” *American Economic Journal: Macroeconomics*, 7, 110–67.
- COCHRANE, J. H. (2011): “Determinacy and Identification with Taylor Rules,” *Journal of Political Economy*, 119, 565 – 615.

- (2015): “The New-Keynesian Liquidity Trap,” *Manuscript, Chicago Booth School of Business*.
- CUBA-BORDA, P. (2014): “What Explains the Great Recession and the Slow Recovery?” *Manuscript, Federal Reserve Board*.
- DEL NEGRO, M., M. P. GIANNONI, AND F. SCHORFHEIDE (2015): “Inflation in the Great Recession and New Keynesian Models,” *American Economic Journal: Macroeconomics*, 7, 168–196.
- DEL NEGRO, M., R. HASEGAWA, AND F. SCHORFHEIDE (2016): “Dynamic Prediction Pools: An Investigation of Financial Frictions and Forecasting Performance,” *Journal of Econometrics*, forthcoming.
- EGGERTSSON, G. B. (2011): “What fiscal policy is effective at zero interest rates?” in *NBER Macroeconomics Annual 2010*, ed. by D. Acemoglu and M. Woodford, University of Chicago Press, vol. 25, 59–112.
- EGGERTSSON, G. B. AND M. WOODFORD (2003): “The Zero Bound on Interest Rates and Optimal Monetary Policy,” *Brookings Papers on Economic Activity*, 2003, 139–211.
- FERNALD, J. (2012): “A quarterly, utilization-adjusted series on total factor productivity,” *Federal reserve bank of San Francisco working paper*, 19, 2012.
- FERNÁNDEZ-VILLAYERDE, J., G. GORDON, P. GUERRÓN-QUINTANA, AND J. F. RUBIO-RAMÍREZ (2015): “Nonlinear Adventures at the Zero Lower Bound,” *Journal of Economic Dynamics and Control*, 57, 182 – 204.
- GUST, C., D. LOPEZ-SALIDO, AND M. E. SMITH (2012): “The Empirical Implications of the Interest-Rate Lower Bound,” *Manuscript, Federal Reserve Board*.
- HERBST, E. AND F. SCHORFHEIDE (2015): *Bayesian Estimation of DSGE Models*, Princeton University Press.
- HIROSE, Y. (2014): “An Estimated DSGE Model with a Deflation Steady State,” *CAMA Working Paper Series*.



- IRELAND, P. N. (2004): “Money’s Role in the Monetary Business Cycle,” *Journal of Money, Credit and Banking*, 36, 969–983.
- ITO, T. AND F. S. MISHKIN (2006): “Two Decades of Japanese Monetary Policy and the Deflation Problem,” in *Monetary Policy under Very Low Inflation in the Pacific Rim*, ed. by T. Ito and A. Rose, University of Chicago Press, vol. NBER-EASE, Volume 15, 131–202.
- JUDD, K. L. (1992): “Projection Methods for Solving Aggregate Growth Models,” *Journal of Economic Theory*, 58, 410 – 452.
- JUDD, K. L., L. MALIAR, AND S. MALIAR (2010): “A Cluster-Grid Projection Method: Solving Problems with High Dimensionality,” *NBER Working Paper*, 15965.
- KRUEGER, D. AND F. KUBLER (2004): “Computing Equilibrium in OLG Models with Production,” *Journal of Economic Dynamics and Control*, 28, 1411–1436.
- KURODA, S. AND I. YAMAMOTO (2008): “Estimating The Frisch Labor Supply Elasticity in Japan,” *Journal of the Japanese and International Economies*, 22, 566–585.
- LUBIK, T. A. AND F. SCHORFHEIDE (2004): “Testing for Indeterminacy: An Application to U.S. Monetary Policy,” *American Economic Review*, 94, 190–217.
- MALIAR, L. AND S. MALIAR (2015): “Merging Simulation and Projection Approaches to Solve High-Dimensional Problems with an Application to a New Keynesian Model,” *Quantitative Economics*, 6, 1–47.
- MAVROEIDIS, S. (2010): “Monetary Policy Rules and Macroeconomic Stability: Some New Evidence,” *American Economic Review*, 100, 491–503.
- MERTENS, K. AND M. O. RAVN (2014): “Fiscal Policy in an Expectations Driven Liquidity Trap,” *The Review of Economic Studies*, 81, 1637–1667.
- PIAZZA, R. (2016): “Self-Fulfilling Deflations,” *Journal of Economic Dynamics and Control*, 73, 18 – 40.

RÍOS-RULL, J.-V., F. SCHORFHEIDE, C. FUENTES-ALBERO, M. KRYSHKO, AND R. SANTAEULALIA-LLOPIS (2012): “Methods versus Substance: Measuring the Effects of Technology Shocks,” *Journal of Monetary Economics*, 59, 826–846.

SCHMITT-GROHÉ, S. AND M. URIBE (2015): “Liquidity Traps and Jobless Recoveries,” *Manuscript, Columbia University*.

SCHORFHEIDE, F. (2008): “DSGE Model-Based Estimation of the New Keynesian Phillips Curve,” *Federal Reserve Bank of Richmond Economic Quarterly*, Fall Issue, 397–433.

UEDA, K. (2012): “The Effectiveness of Non-Traditional Monetary Policy Measures: The Case of the Bank of Japan,” *The Japanese Economic Review*, 63(1), 1–22.

WOODFORD, M. (2003): *Interest and Prices*, Princeton University Press.

# **Online Appendix to “Macroeconomic Dynamics Near the ZLB: A Tale of Two Countries”**

**S. Boragan Aruoba, Pablo Cuba-Borda, and Frank Schorfheide**

This Appendix consists of six sections:

- A. Solving the Two-Equation Model of Section 2
- B. Equilibrium Conditions for the Model of Section 3
- C. Model Solution Algorithm
- D. Data
- E. DSGE Model Estimation
- F. Particle Filter For Sunspot Equilibrium

## A Solving the Two-Equation Model of Section 2

Here we define  $\hat{r}_t = -\hat{M}_t$ . The model is characterized by the nonlinear difference equation

$$\mathbb{E}_t [\hat{\pi}_{t+1}] = \max \left\{ -\log(r\pi_*) - \rho\hat{r}_t, \psi\hat{\pi}_t - \rho\hat{r}_t \right\} \quad (\text{A.1})$$

We assume that  $r\pi_* \geq 1$  and  $\psi > 1$ .

**The Targeted-Inflation Equilibrium.** Consider a solution to (A.1) that takes the following form

$$\hat{\pi}_t = \theta_0 + \theta_1 \hat{r}_t \quad (\text{A.2})$$

We now determine values of  $\theta_0$  and  $\theta_1$  such that (A.1) is satisfied. We begin by calculating the following expectation

$$\begin{aligned} \mathbb{E}_t [\hat{\pi}_{t+1}] &= \mathbb{E}_t [\theta_0 + \theta_1 \hat{r}_{t+1}] \\ &= \theta_0 + \theta_1 \rho \hat{r}_t \end{aligned}$$

Combining this expression with (A.1) yields

$$\theta_0 + \theta_1 \rho \hat{r}_t = \max \left\{ -\log(r\pi_*) - \rho\hat{r}_t, \psi\theta_0 + (\psi\theta_1 - \rho)\hat{r}_t \right\} \quad (\text{A.3})$$

The targeted-inflation equilibrium is obtained by equating the left-hand side of (A.3) with the second term in the right-hand-side max-operator, which leads to

$$\theta_0^* = 0, \quad \theta_1^* = \frac{\rho}{\psi - \rho}. \quad (\text{A.4})$$

The derivation is completed by noting that in the targeted-inflation equilibrium the second term in the max operator in (A.3) is greater than the first term:

$$\frac{\psi\rho}{\psi - \rho} \hat{r}_t \geq -\log(r\pi_*), \quad (\text{A.5})$$

provided that  $\sigma$  is small and thus  $\hat{r}_t \approx 0$ . Because  $\psi > 1$ , there is a locally unique stable

targeted-inflation equilibrium.

**Deflation Equilibria.** A deflation equilibrium is obtained by equating the left-hand side of (A.3) with the first term in the right-hand-side max-operator, which leads to

$$\theta_0^D = -\log(r\pi_*), \quad \theta_1^D = -1, \quad (\text{A.6})$$

The derivation is completed by noting that under this solution the first term in the max operator in (A.3) is greater than the second term:

$$(\psi - 1) \log(r\pi_*) \geq -\psi \hat{r}_t, \quad (\text{A.7})$$

provided that  $\sigma$  is sufficiently small and thus  $\hat{r}_t \approx 0$ .

Locally around the deflation steady state, interest rates do not respond to inflation rates and it is well-known that the system is locally indeterminate. This suggests that we can construct alternative solutions to (A.1). Consider the following conjecture for inflation which is a generalized version of (A.2)

$$\hat{\pi}_t^D = -\log(r\pi_*) + \theta_1^D \hat{r}_t + \theta_2^D \hat{r}_{t-1} + \theta_3^D \zeta_t, \quad (\text{A.8})$$

where we allow the solution to depend on  $\hat{r}_{t-1}$ , and a sunspot variable  $\zeta_t$  which has the property  $\mathbb{E}_{t-1}[\zeta_t] = 0$ .

Under this conjecture, the expected inflation becomes

$$\mathbb{E}_t[\hat{\pi}_{t+1}^D] = \mathbb{E}_t[-\log(r\pi_*) + \theta_1^D \hat{r}_{t+1} + \theta_2^D \hat{r}_t + \theta_3^D \zeta_{t+1}] \quad (\text{A.9})$$

$$= -\log(r\pi_*) + (\rho\theta_1^D + \theta_2^D) \hat{r}_t \quad (\text{A.10})$$

Assuming once again that this expectation is equal to the first term in the max operator, we need to solve

$$-\log(r\pi_*) + (\rho\theta_1^D + \theta_2^D) \hat{r}_t = -\log(r\pi_*) - \rho \hat{r}_t \quad (\text{A.11})$$

which requires  $\rho\theta_1^D + \theta_2^D = -\rho$ . This shows that there are two indeterminacies. First, the

value of  $\theta_3^D$  is arbitrary. Second, for any choice of  $\theta_2^D$  we can find a  $\theta_1^D$  that is a valid solution. In the main text we set  $\theta_3^D = 0$  and chose  $\theta_2^D = 0$  to yield  $\theta_1^D = -1$ , but clearly a continuum of other values are admissible.

**A Sunspot Equilibrium.** Let  $s_t \in \{0, 1\}$  denote the Markov-switching sunspot process. Assume the system is in the targeted-inflation regime if  $s_t = 1$  and that it is in the deflation regime if  $s_t = 0$ . The probabilities of staying in state 0 and 1, respectively, are denoted by  $p_{00}$  and  $p_{11}$ . We conjecture that the inflation dynamics follow the process

$$\hat{\pi}_t^{(s)} = \theta_0(s_t) + \theta_1(s_t)\hat{r}_t. \quad (\text{A.12})$$

In this case condition (A.3) turns into

$$\begin{aligned} [p_{11}\theta_0(1) + (1 - p_{11})\theta_0(0)] + \rho[p_{11}\theta_1(1) + (1 - p_{11})\theta_1(0)]\hat{r}_t &= \psi(\theta_0(1) + \theta_1(1)\hat{r}_t) - \rho\hat{r}_t \\ [p_{00}\theta_0(0) + (1 - p_{00})\theta_0(1)] + \rho[p_{00}\theta_1(0) + (1 - p_{00})\theta_1(1)]\hat{r}_t &= -\log(r\pi_*) - \rho\hat{r}_t \end{aligned}$$

which yield a system of four linear equations by collecting the constants and slopes of each side, in the four unknowns,  $(\theta_0(0), \theta_1(0), \theta_0(1), \theta_1(1))$  that can easily be solved numerically. To complete the solution, we need to verify that under the solutions we found, the right-side of the max operator is active in the  $s = 1$  solution, and the left-side is active in the  $s = 0$  solution. This requires checking

$$\psi\theta_0(1) + (\psi\theta_1(1) - \rho)\hat{r}_t \geq -\log(r\pi_*) - \rho\hat{r}_t \quad (\text{A.13})$$

$$-\log(r\pi_*) - \rho\hat{r}_t \geq \psi\theta_0(0) + (\psi\theta_1(0) - \rho)\hat{r}_t \quad (\text{A.14})$$

when  $\hat{r}_t \approx 0$  which would hold when  $\sigma$  is small.

## B Equilibrium Conditions for the Model of Section 3

In this section we sketch the derivation of the equilibrium conditions presented in Section 3.

### B.1 Households

The representative household solves

$$\max_{\{C_{t+s}, H_{t+s}, B_{t+s}, M_{t+s}\}} \mathbb{E}_t \left[ \sum_{s=0}^{\infty} \beta^s d_{t+s} \left( \frac{(C_{t+s}/A_{t+s})^{1-\tau} - 1}{1-\tau} - \chi_H \frac{H_{t+s}^{1+1/\eta}}{1+1/\eta} + \chi_M V \left( \frac{M_{t+s}}{P_{t+s} A_{t+s}} \right) \right) \right],$$

subject to:

$$P_t C_t + T_t + B_t + M_t = P_t W_t H_t + M_{t-1} + R_{t-1} B_{t-1} + P_t D_t + P_t S C_t,$$

**Consumption and bond holdings.** Let  $\beta^s d_{t+s} \lambda_{t+s}$  be the Lagrange multiplier on the household budget constraint. Then the first-order condition with respect to consumption and bond holdings are given by:

$$\begin{aligned} P_t \lambda_t &= \left( \frac{C_t}{A_t} \right)^{-\tau} \frac{1}{A_t} \\ \lambda_t &= \beta \frac{d_{t+1}}{d_t} R_t \lambda_{t+1}. \end{aligned}$$

Combining the two equation of the bond holding first order condition, leads to the consumption Euler equation:

$$1 = \beta \mathbb{E}_t \left[ \frac{d_{t+1}}{d_t} \left( \frac{C_{t+1}/A_{t+1}}{C_t/A_t} \right)^{-\tau} \frac{1}{\gamma z_{t+1}} \frac{R_t}{\pi_{t+1}} \right],$$

where  $\gamma z_{t+1} = A_{t+1}/A_t$ . We define the stochastic discount factor as:

$$Q_{t+1|t} = \frac{d_{t+1}}{d_t} \left( \frac{C_{t+1}/A_{t+1}}{C_t/A_t} \right)^{-\tau} \frac{1}{\gamma z_{t+1}}.$$

**Labor-Leisure Choice.** Taking first-order conditions with respect to  $H_t$  yields the standard intratemporal optimality condition for the allocation of labor

$$\frac{W_t}{A_t} = \chi_H \left( \frac{C_t}{A_t} \right)^\tau H_t^{1/\eta}.$$

## B.2 Intermediate Goods Firms

Each intermediate good producer buys labor services  $H_t(j)$  at the real wage  $W_t$ . Firms face nominal rigidities in terms of price adjustment costs. The adjustment cost, expressed as a fraction of firms' real output, is given by the function  $\Phi_p \left( \frac{P_t(j)}{P_{t-1}(j)} \right)$ . We assume that the adjustment cost function is twice-continuously differentiable, weakly increasing and weakly convex,  $\Phi'_p \geq 0$  and  $\Phi''_p \geq 0$ . The firm maximizes expected discounted real profits with respect to  $H_t(j)$  and  $P_t(j)$ :

$$\mathbb{E}_t \sum_{s=0}^{\infty} \beta^s Q_{t+s|t} \left( \frac{P_{t+s}(j)}{P_{t+s}} A_{t+s} H_{t+s}(j) - \Phi_p \left( \frac{P_{t+s}(j)}{P_{t+s-1}(j)} \right) A_{t+s} H_{t+s}(j) - W_{t+s} H_{t+s}(j) \right),$$

subject to

$$A_t H_t(j) = \left( \frac{P_t(j)}{P_t} \right)^{-1/\nu} Y_t.$$

We use  $\mu_{t+s} \beta^s Q_{t+s|t}$  to denote the Lagrange multiplier associated with this constraint. In equilibrium, the firms use the households' stochastic discount factor to discount future profits.

**Price setting decision.** Setting  $Q_{t|t} = 1$ , the first-order condition with respect to  $P_t(j)$  is given by:

$$\begin{aligned} 0 = & \frac{A_t H_t(j)}{P_t} - \Phi'_p \left( \frac{P_t(j)}{P_{t-1}(j)} \right) \frac{A_t H_t(j)}{P_{t-1}(j)} - \frac{\mu_t}{\nu} \left( \frac{P_t(j)}{P_t} \right)^{-1/\nu-1} \frac{Y_t}{P_t} \\ & + \beta \mathbb{E}_t \left[ Q_{t+1|t} \Phi'_p \left( \frac{P_{t+1}(j)}{P_t(j)} \right) A_{t+1} H_{t+1}(j) \frac{P_{t+1}(j)}{P_t^2(j)} \right]. \end{aligned}$$



**Firms' labor demand.** Taking first-order conditions with respect to  $H_t(j)$  yields

$$W_t = \frac{P_t(j)}{P_t} A_t - \Phi_p \left( \frac{P_t(j)}{P_{t-1}(j)} \right) A_t - \mu_t A_t.$$

**Symmetric equilibrium.** We restrict attention to a symmetric equilibrium where all firms choose the same price  $P_t(j) = P_t \forall j$ . This assumption implies that in equilibrium all firms face identical marginal costs and demand the same amount of labor input. Combining the firms' price setting and labor demand first order conditions and assuming that the price adjustment costs are quadratic, i.e.,

$$\Phi_p \left( \frac{P_t(j)}{P_{t-1}(j)} \right) = \frac{\phi}{2} \left( \frac{P_t(j)}{P_{t-1}(j)} - \bar{\pi} \right)^2,$$

we obtain:

$$(1 - \nu) - \chi_H \left( \frac{C_t}{A_t} \right)^\tau H_t^{1/\eta} - \frac{\phi}{2} \left( \frac{P_t}{P_{t-1}} - \bar{\pi} \right) + \nu \phi \left( \frac{P_t}{P_{t-1}} - \bar{\pi} \right) \frac{P_t}{P_{t-1}} = \nu \beta \mathbb{E}_t \left[ Q_{t+1|t} \frac{P_{t+1}}{P_t} \Phi'_p \left( \frac{P_{t+1}}{P_t} \right) \frac{Y_{t+1}}{Y_t} \right].$$

### B.3 Equilibrium Conditions

**Resource constraint.** The derivation of the aggregate resource constraint is straightforward. In equilibrium real profits by intermediate producers is given by:

$$D_t = Y_t - \Phi_p(\pi_t) Y_t - W_t H_t$$

Substituting this into the household budget constraint we obtain:

$$C_t + \left[ \frac{T_t}{P_t} + \frac{M_t}{P_t} + \frac{B_t}{P_t} - \frac{M_{t-1}}{P_t} - \frac{R_{t-1} B_{t-1}}{P_t} \right] = W_t H_t + Y_t - \Phi_p(\pi_t) Y_t - W_t H_t$$

From the government budget constraint in (21) we can see that the term in square brackets corresponds to real government expenditure  $G_t$ . Simplifying yields:

$$C_t + G_t = [1 - \Phi_p(\pi_t)] Y_t$$

The technology process introduces a long-run trend in the variables of the model. To make the model stationary we use the following transformations:  $y_t = Y_t/A_t$ ,  $c_t = C_t/A_t$ , and note that  $Y_t/Y_{t-1} = \frac{y_t}{y_{t-1}}\gamma z_t$ . We also define the gross inflation rate  $\pi_t = P_t/P_{t-1}$ . The equilibrium conditions shown in the main text follow immediately:

## C Model Solution Algorithm

### Algorithm 1 (Model Solution)

1. Start with a guess for  $\Theta$ . For the targeted-inflation regime ( $s_t = 1$ ), this guess is obtained from a first-order linear approximation around the targeted-inflation steady state. For the deflation regime ( $s_t = 0$ ), it is obtained by assuming constant decision rules for inflation and  $\mathcal{E}$  at the deflation steady state.
2. Given this guess, simulate the sunspot model for a large number of periods. This simulation also includes the simulated path of the sunspot variable  $s_t$ . We use 10,000 simulations after a burn-in period of 150 observations.
3. Given the simulated path, obtain the grid for the state variables over which the approximation needs to be accurate. We use a time-separated grid algorithm, that is we sample from the simulation at fixed intervals to deliver the grid points that represent the ergodic set. For a fourth order approximation we construct the ergodic distribution setting  $M = 880$  for both countries and obtain 50% of these points conditioning on  $s_t = 1$  and the remaining are conditioned on  $s_t = 0$ . This grid oversamples points from the  $s_t = 0$  regime to increase the accuracy of the solution.
  - (a) For the U.S. we replace 356 grid points of the ergodic grid with filtered states. We use 36 filtered states corresponding to the period 2000:Q1-2008Q4, 160 points corresponding to filtered states, using multiple particles per period from 2009:Q1-2015:Q2 conditioning on  $s_t = 1$ , and 160 points corresponding to filtered states using multiple particles per period from 2009:Q1-2009:Q4 conditioning on  $s_t = 0$ .
  - (b) For Japan we replace 260 grid points of the ergodic grid with filtered states using multiple particles per period from 1999:Q1 - 2015:Q1. We obtain 50% of these filtered states forcing  $s_t = 1$  and the remaining 50% forcing  $s_t = 0$ .
4. Solve for the  $\Theta$  by minimizing the sum of squared residuals using Algorithm 2 and a standard nonlinear solver.

5. Repeat steps 2-4 a sufficient number of times so that both the ergodic distribution of the sunspot model and the filtered states used in the solution grid remain unchanged from one iteration to the next.

**Algorithm 2 (Determinining the Approximate Decision Rules)**

1. For a generic grid point  $\mathcal{S}_i$  and the current value for  $\Theta$ , compute  $f_\pi^1(\mathcal{S}_i; \Theta)$ ,  $f_\pi^2(\mathcal{S}_i; \Theta)$ ,  $f_\mathcal{E}^1(\mathcal{S}_i; \Theta)$ , and  $f_\mathcal{E}^2(\mathcal{S}_i; \Theta)$ .
2. Assume  $\zeta_i \equiv I\{R(\mathcal{S}_i, \Theta) > 1\} = 1$  and compute  $\pi_i$ , and  $\mathcal{E}_i$ , as well as  $c_i$  and  $y_i$  using (26) and (29).
3. Compute  $R_i$  based on (16) using  $\pi_i$  and  $y_i$  obtained in Step 2. If  $R_i$  is greater than unity, then  $\zeta_i$  is indeed equal to one. Otherwise, set  $\zeta_i = 0$  (and thus  $R_i = 1$ ) and recompute all other objects.
4. The final step is to compute the residual functions. In each regime  $s_t = \{0, 1\}$  there are four residuals, corresponding to the four functions being approximated. For a given set of state variables  $\mathcal{S}_i$ , only two of them will be relevant since we either need the constrained decision rules or the unconstrained ones. Taking into account the transition of the sunspot the residual functions will be given by

$$\mathcal{R}^1(\mathcal{S}_i) = \mathcal{E}_i - \iiint \frac{d'}{d} \frac{c(\mathcal{S}')^{-\tau}}{\gamma z' \pi(\mathcal{S}')} dF(d') dF(g') dF(z') dF(\epsilon'_R) dF(s') \quad (\text{A.15})$$

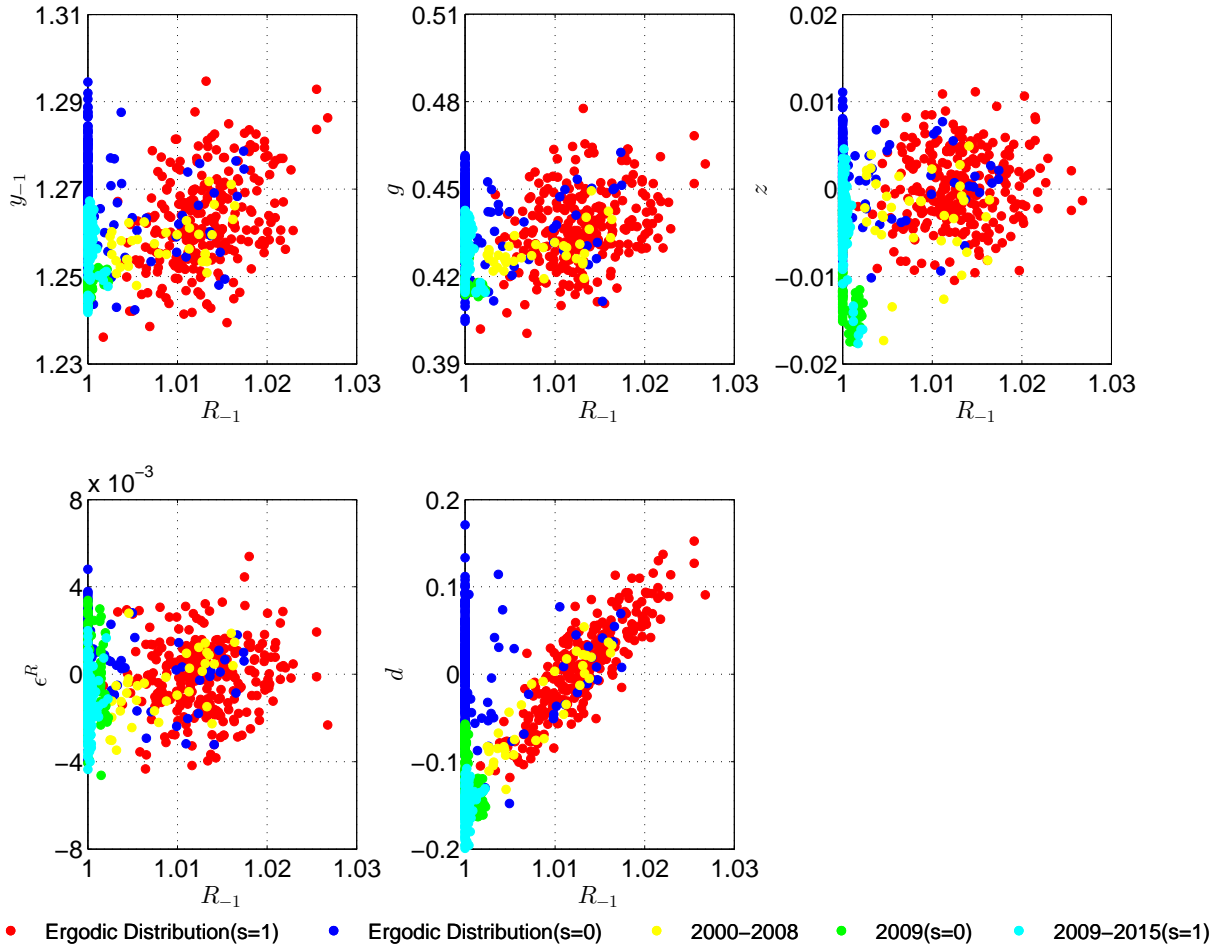
$$\begin{aligned} \mathcal{R}^2(\mathcal{S}_i) &= \xi(c_i, \pi_i, y_i) \\ &- \phi \beta \iiint \frac{d'}{d} c(\mathcal{S}')^{-\tau} y(\mathcal{S}') [\pi(\mathcal{S}') - \bar{\pi}] \pi(\mathcal{S}') dF(d') dF(g') dF(z') dF(\epsilon'_R) dF(s') \end{aligned} \quad (\text{A.16})$$

where

$$\xi(c_i, \pi_i, y_i) \equiv c_i^{-\tau} y_i \left\{ \frac{1}{\nu} \left( 1 - \chi_h c_i^\tau y_i^{1/\eta} \right) + \phi(\pi_i - \bar{\pi}) \left[ \left( 1 - \frac{1}{2\nu} \right) \pi_i + \frac{\bar{\pi}}{2\nu} \right] - 1 \right\}.$$

Note that this step involves computing  $\pi(\mathcal{S}')$ ,  $y(\mathcal{S}')$ ,  $c(\mathcal{S}')$ , and  $R(\mathcal{S}')$  which is done following steps 1-3 above for each value of  $\mathcal{S}'$ . We use a non-product monomial integration rule to evaluate these integrals. The integrals are written to accommodate the

Figure A-1: Solution Grid for the Sunspot Equilibrium - 4vGrowth U.S.

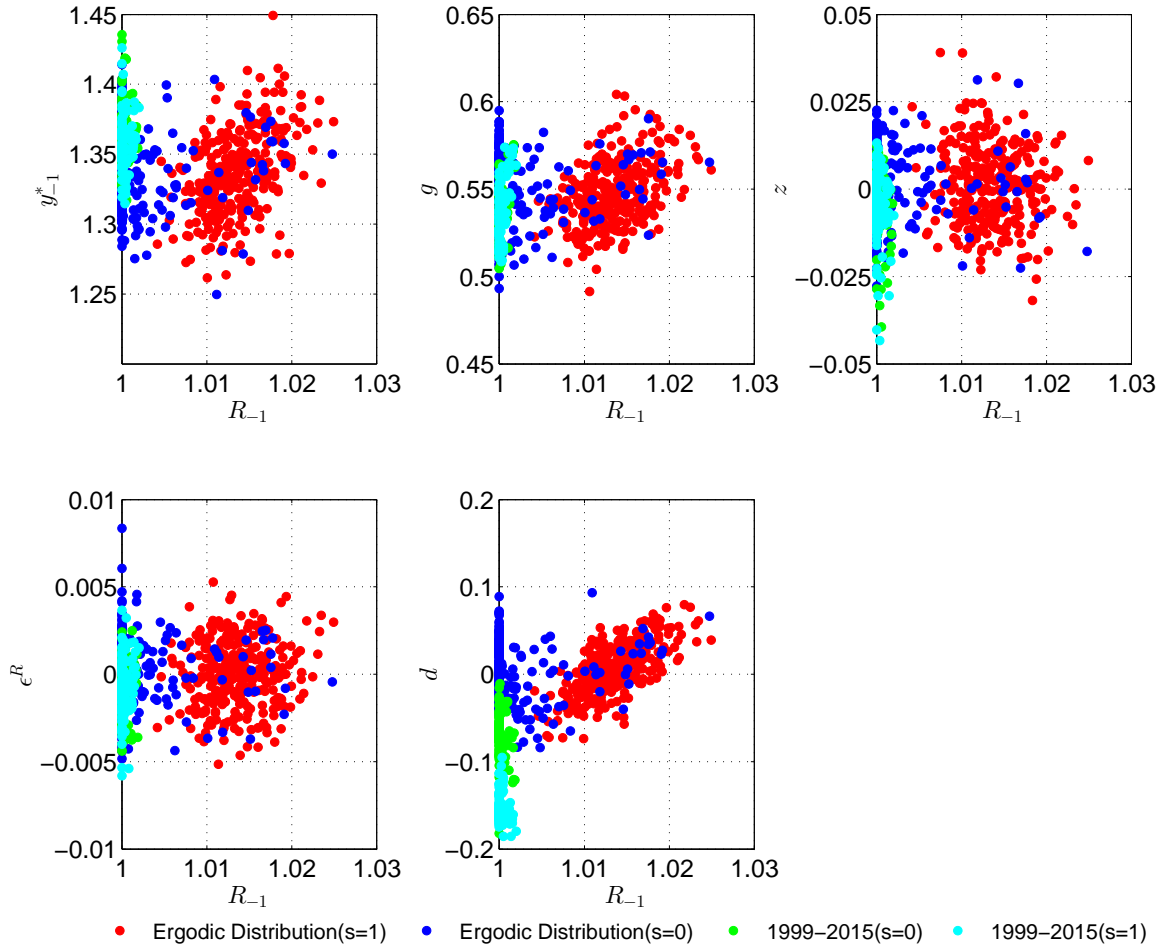


4-variable versions and when the discount factor shock isn't in the model we drop the integration with respect to  $d$ .

5. The objective function to be minimized is the sum of squared residuals obtained in Step 4.

We use analytical derivatives of the objection function, which speeds up the solution by two orders of magnitude. As a measure of accuracy, we compute the approximation errors from (A.15) and (A.16), converted to consumption units. The approximation errors are in the order of  $10^{-4}$  on average.

Figure A-2: Solution Grid for the Sunspot Equilibrium - 4vGap Japan



Figures A-1 and A-2 show the solution grid for the sunspot equilibrium for 4vGrowth model for the U.S. and 4vGap model for Japan. For each panel, we have  $R_{t-1}$  on the  $x$  axis and one of the other exogenous state variables on the  $y$  axis. The red (blue) dots are the grid points that represent the ergodic distribution conditional on  $s_t = 1$  ( $s_t = 0$ ). For both countries we include filtered grid points used in the construction of the grid. For the U.S. the yellow dots denote filtered states between 2000 to 2008; the green dots represent filtered states from 2009 conditioning on  $s_t = 0$  and the turquoise dots represent filtered states from 2009 to 2015 conditioning on  $s_t = 1$ . For Japan the green (turquoise) dots represent filtered states from 1999 to 2015 conditioning on  $s_t = 0$  ( $s_t = 1$ ). In both cases the filtered states lie in the tails of the ergodic distribution of the sunspot equilibrium. By adding these

filtered states to the grid points, we ensure that our approximation will be accurate in these low-probability regions.

The decision rule  $\pi^e(\cdot)$  for inflation expectations is obtained as follows. Using the same grid points  $\mathcal{S}_i$  as for the above model solution, we use the Monte Carlo approximation described in the main text to obtain  $\hat{\pi}^e(\mathcal{S}_i)$ . We then find the coefficients for the Chebyshev polynomial approximation of the function  $\pi^e(\mathcal{S}_t)$  by minimizing the squared differences between the series approximation and the simulation approximation at the grid points  $\mathcal{S}_i$ .

## D Data

### D.1 United States

**Real per capita GDP:** We obtain real GDP (GDPC96) and convert into per capita terms using the Civilian Noninstitutional Population (CNP16OV). We smooth the population series applying an eight-quarter backward-looking moving average filter. Source: FRB St. Louis FRED database.

**Real per capita consumption:** We obtain real personal consumption expenditures (PCECC96) and convert into per capita terms using the Civilian Noninstitutional Population (CNP16OV). Source: FRED.

**Real per capita government consumption:** We obtain real government consumption expenditures and gross investment (GCEC1) and convert into per capita terms using the Civilian Noninstitutional Population (CNP16OV). Source: FRED.

**GDP Deflator Inflation:** Log difference of GDP deflator (GDPDEF), multiplied by 400 to convert it into annualized percentages. Source: FRED.

**Interest Rate / Monetary Policy Rate:** Effective federal funds rate (FEDFUNDS) averaged over each quarter. Source: FRED.

**Potential GDP:** We use real potential GDP (GDPPOT) produced by the U.S. Congressional Budget Office. Source: FRED.

**Inflation Expectations:** Monthly 10-year-ahead inflation expectations from Aruoba (2014) averaged within each quarter.

### D.2 Japan

**Real per capita GDP:** We collect real GDP (RGDP) from the Cabinet Office's National Accounts. We use the statistical release of benchmark year 2005 that covers the period 1994:Q1 - 2015:Q1. To extend the sample we collect RGDP figures from the benchmark year 2000 and construct a series spanning the period 1981:Q1-2015:Q1 using the quarterly growth rate of the RGDP benchmark year 2000. Our measure of per-capita output is RGDP divided by the total population of 15 years and over. We smooth the quarterly growth of the



population series using an eight quarter backward-looking moving average filter. We obtain population data from the Statistics Bureau of the Ministry of Foreign Affairs Historical data Table b-1.

**Real per capita consumption:** We collect real private consumption data from the Cabinet Office's National Accounts and follow the same procedure as for real GDP to convert it into per capita terms.

**Real per capita government consumption:** We collect real government consumption and public investment data from the Cabinet Office's National Accounts and follow the same procedure as for real GDP to convert it into per capita terms.

**GDP deflator inflation:** Log difference of GDP deflator, multiplied by 400 to convert it into annualized percentages. We use the implicit GDP deflator index from the Cabinet Office. We also extend the benchmark year 2005 release using the growth rate of the index from the benchmark year 2000 figures.

**Interest Rate / Monetary Policy Rate:** For the nominal interest rate we use the Bank of Japan's uncollateralized call rate (STSTRACLUCON) from 1986:M7-2015:M3. To complete the series from 1981.M1 - 1985.M6 we use the monthly average of the collateralized overnight call rate (STSTRACLCOON). Finally we transform monthly figures using quarterly averages over the sample period.

**Potential GDP:** We construct a measure of potential GDP using the output gap estimated by the Bank of Japan and semi-annual potential growth rates from the Cabinet Office. We set our measure of potential GDP equal to observed real GDP in 1981.Q1.

**Inflation Expectations:** 6-to-10-year-ahead inflation forecasts from the G7 Long-term Forecasts of Consensus Economics

([http://www.consensuseconomics.com/download/G7\\_Economic\\_Forecasts.htm](http://www.consensuseconomics.com/download/G7_Economic_Forecasts.htm)). This is a survey-based measure based on professional forecasters. Long-term forecasts are released in April and October of every year. To construct quarterly series we use linear interpolation.

Table A-1: Parameters Fixed During Estimation

Parameter	US					
	3vGrowth	4vGrowth-C	4vGrowth-G	3vGap	4vGap-C	4vGap-G
$400 \ln(r^*)$	0.86	0.86	0.86	0.86	0.86	0.86
$400 \ln(\pi^*)$	2.72	2.46	2.38	2.46	2.46	2.35
$100 \ln(\gamma)$	0.50	0.50	0.50	0.50	0.50	0.50
$g_*$	1.54	1.54	1.28	1.54	1.54	1.28
$\nu$	0.10	0.10	0.10	0.10	0.10	0.10
$\eta$	0.72	0.72	0.72	0.72	0.72	0.72
$\alpha$				0.90	0.90	0.90

Parameter	Japan					
	3vGrowth	4vGrowth-C	4vGrowth-G	3vGap	4vGap-C	4vGap-G
$400 \ln(r^*)$	1.88	1.88	1.88	1.88	1.88	1.88
$400 \ln(\pi^*)$	1.27	1.25	1.25	1.28	1.27	1.25
$100 \ln(\gamma)$	0.56	0.56	0.56	0.56	0.56	0.56
$g_*$	1.72	1.72	1.28	1.72	1.72	1.28
$\nu$	0.10	0.10	0.10	0.10	0.10	0.10
$\eta$	0.85	0.85	0.85	0.85	0.85	0.85
$\alpha$				0.85	0.85	0.85

*Notes:* The steady state ratio  $g_* = (c/y)^{-1}$ . The sunspot shock transition probability parameters  $p_{00}$  and  $p_{11}$  do not affect the estimation because it is based on a first-order perturbation approximation of the targeted-inflation equilibrium.

## E DSGE Model Estimation

### E.1 Priors for estimation

Table A-1 lists the parameters that were fixed during the estimation. Marginal prior distributions the remaining DSGE model parameters are summarized in Table A-2. We assume that the parameters are *a priori* independent. Thus, the joint prior distribution is given by the product of the marginals. We truncate the joint distribution to ensure local determinacy of the targeted inflation equilibrium. For the 3-variable specifications we used alternative priors for  $\psi_1$  and  $\psi_2$ , which are summarized in Table A-3.

Table A-2: Benchmark Priors for Estimation

Parameter	Description	Density	US		Japan	
			P(1)	P(2)	P(1)	P(2)
$\tau$	Inverse IES	$\mathcal{G}$	2.0	.25	2.0	0.5
$\kappa$	Slope (linearized) Phillips curve	$\mathcal{G}$	0.3	0.1	0.3	0.1
$\psi_1$	Taylor rule: weight on inflation	$\mathcal{G}$	1.5	0.3	1.5	0.3
$\psi_2$	Taylor rule: weight on output	$\mathcal{G}$	0.5	.25	0.5	.25
$\rho_r$	Interest rate smoothing	$\mathcal{B}$	0.5	0.2	0.6	0.2
$\rho_g$	Persistence: demand shock	$\mathcal{B}$	0.8	0.1	0.6	0.2
$\rho_z$	Persistence: technology shock	$\mathcal{B}$	0.2	0.1	0.6	0.2
$\rho_d$	Persistence: discount factor shock	$\mathcal{B}$	0.8	0.1	0.6	0.2
$100\sigma_r$	Std dev: monetary policy shock	$\mathcal{IG}$	0.3	4.0	0.3	4.0
$100\sigma_g$	Std dev: demand shock	$\mathcal{IG}$	0.4	4.0	0.4	4.0
$100\sigma_z$	Std dev: technology shock	$\mathcal{IG}$	0.4	4.0	0.4	4.0
$100\sigma_d$	Std dev: discount factor shock	$\mathcal{IG}$	0.4	4.0	0.4	4.0

Notes:  $\mathcal{G}$  is Gamma distribution;  $\mathcal{B}$  is Beta distribution; and  $\mathcal{IG}$  is Inverse Gamma distribution. P(1) and P(2) are the mean and the standard deviations for Beta and Gamma distributions;  $s$  and  $\nu$  for the Inverse Gamma distribution, where  $p_{\mathcal{IG}}(\sigma|\nu, s) \propto \sigma^{-\nu-1} e^{-\nu s^2/2\sigma^2}$ .

Table A-3: Modified Priors for 3-Variable Models

Parameter	Description	Density	US		Japan	
			P(1)	P(2)	P(1)	P(2)
3vGrowth Specification						
$\psi_1$	Taylor rule: weight on inflation	$\mathcal{G}$	1.50	0.05	1.50	0.15
$\psi_2$	Taylor rule: weight on output	$\mathcal{G}$	0.80	0.01	(Benchm.)	
3vGap Specification						
$\psi_1$	Taylor rule: weight on inflation	$\mathcal{G}$	2.55	0.05	1.70	0.05
$\psi_2$	Taylor rule: weight on output	$\mathcal{G}$	0.35	0.01	0.15	0.01

Notes:  $\mathcal{G}$  is Gamma distribution.

## E.2 Posterior Simulator

We estimate a first-order approximation of the targeted-inflation equilibrium of the DSGE model, ignoring the presence of the ZLB. Thus, the likelihood function can be evaluated with the Kalman filter which speeds up the estimation. For the the output growth specifications we initialize the initial level of technology,  $A_0$ , in the Kalman filter such that  $\log Y_1$  is identical to the data in the first quarter of our estimation sample. All other states are initialized using

their unconditional distribution. For the output gap specifications we initialize  $A_0$  such that if we use  $\log Y_t$  as observable the model tracks  $\log Y_t^*$  computed from actual output data.

Draws from the posterior distribution are generated using the random walk Metropolis algorithm (RWM) described in An and Schorfheide (2007). The covariance matrix of the proposal distribution is scaled such that the RWM algorithm has an acceptance rate of approximately 50%. We generate 100,000 draws from the posterior distribution and discard the first 50,000 draws. Summary statistics of the posterior distribution are based on the last 50,000 draws of the sequence.

Table A-4: Posterior of DSGE Model Parameters

Parameter	US											
	3vGrowth		4vGrowth-C		4vGrowth-G		3vGap		4vGap-C		4vGap-G	
$\tau$	1.92	(1.56, 2.33)	2.10	(1.72, 2.51)	2.01	(1.63, 2.42)	2.03	(1.66, 2.47)	2.28	(1.90, 2.68)	2.16	(1.76, 2.59)
$\kappa$	0.26	(0.17, 0.38)	0.31	(0.20, 0.44)	0.22	(0.13, 0.33)	0.32	(0.18, 0.50)	0.27	(0.14, 0.44)	0.21	(0.10, 0.38)
$\psi_1$	1.47*	(1.38, 1.56)*	2.67	(2.21, 3.17)	2.60	(2.14, 3.09)	2.50*	(2.42, 2.58)*	2.55	(2.17, 2.99)	2.65	(2.25, 3.10)
$\psi_2$	0.80*	(0.79, 0.82)*	0.90	(0.61, 1.24)	0.99	(0.68, 1.33)	0.36*	(0.34, 0.37)*	0.35	(0.26, 0.44)	0.32	(0.23, 0.41)
$\rho_r$	0.67	(0.61, 0.73)	0.80	(0.76, 0.84)	0.80	(0.76, 0.84)	0.73	(0.67, 0.78)	0.81	(0.77, 0.84)	0.80	(0.76, 0.84)
$\rho_g$	0.87	(0.84, 0.90)	0.93	(0.88, 0.97)	0.97	(0.95, 0.99)	0.79	(0.75, 0.82)	0.87	(0.82, 0.93)	0.97	(0.95, 0.99)
$\rho_z$	0.10	(0.03, 0.20)	0.16	(0.05, 0.29)	0.19	(0.07, 0.34)	0.09	(0.03, 0.17)	0.36	(0.17, 0.56)	0.23	(0.08, 0.40)
$\rho_d$			0.93	(0.90, 0.96)	0.92	(0.88, 0.95)			0.94	(0.92, 0.97)	0.93	(0.89, 0.96)
$100\sigma_r$	0.22	(0.18, 0.26)	0.16	(0.14, 0.19)	0.16	(0.14, 0.19)	0.19	(0.16, 0.23)	0.14	(0.12, 0.16)	0.14	(0.12, 0.16)
$100\sigma_g$	0.61	(0.51, 0.73)	0.46	(0.41, 0.52)	0.25	(0.23, 0.28)	1.09	(0.94, 1.26)	0.47	(0.42, 0.53)	0.26	(0.23, 0.29)
$100\sigma_z$	0.64	(0.56, 0.74)	0.46	(0.41, 0.52)	0.59	(0.51, 0.67)	0.57	(0.48, 0.68)	0.39	(0.33, 0.45)	0.53	(0.45, 0.61)
$100\sigma_d$			1.84	(1.30, 2.60)	1.72	(1.24, 2.39)			2.47	(1.66, 3.84)	2.31	(1.62, 3.31)

Parameter	Japan											
	3vGrowth		4vGrowth-C		4vGrowth-G		3vGap		4vGap-C		4vGap-G	
$\tau$	0.96	(0.59, 1.45)	1.21	(0.71, 1.84)	0.98	(0.56, 1.53)	1.23	(0.79, 1.79)	1.73	(1.10, 2.48)	1.44	(0.79, 2.23)
$\kappa$	0.48	(0.29, 0.70)	0.48	(0.30, 0.69)	0.41	(0.25, 0.60)	0.55	(0.37, 0.78)	0.39	(0.23, 0.58)	0.33	(0.18, 0.51)
$\psi_1$	1.43*	(1.19, 1.66)*	1.80	(1.43, 2.22)	1.72	(1.35, 2.14)	1.67*	(1.59, 1.75)*	1.69	(1.36, 2.10)	1.73	(1.37, 2.17)
$\psi_2$	0.44	(0.28, 0.64)	0.42	(0.24, 0.63)	0.41	(0.25, 0.60)	0.15*	(0.14, 0.17)*	0.15	(0.09, 0.22)	0.13	(0.07, 0.21)
$\rho_r$	0.64	(0.49, 0.75)	0.73	(0.61, 0.82)	0.69	(0.55, 0.79)	0.73	(0.64, 0.80)	0.78	(0.70, 0.85)	0.78	(0.68, 0.85)
$\rho_g$	0.86	(0.80, 0.91)	0.94	(0.90, 0.98)	0.95	(0.91, 0.99)	0.86	(0.81, 0.90)	0.92	(0.86, 0.97)	0.96	(0.92, 0.99)
$\rho_z$	0.03	(0.01, 0.08)	0.06	(0.02, 0.12)	0.05	(0.02, 0.11)	0.07	(0.02, 0.13)	0.14	(0.04, 0.29)	0.14	(0.04, 0.30)
$\rho_d$			0.90	(0.84, 0.95)	0.90	(0.84, 0.94)			0.90	(0.85, 0.95)	0.90	(0.85, 0.95)
$100\sigma_r$	0.24	(0.18, 0.32)	0.21	(0.16, 0.28)	0.23	(0.17, 0.31)	0.21	(0.17, 0.26)	0.19	(0.15, 0.23)	0.19	(0.15, 0.24)
$100\sigma_g$	0.96	(0.68, 1.34)	0.75	(0.64, 0.88)	0.50	(0.43, 0.58)	1.43	(1.10, 1.87)	0.77	(0.66, 0.90)	0.51	(0.44, 0.60)
$100\sigma_z$	1.22	(1.03, 1.45)	1.10	(0.94, 1.29)	1.27	(1.08, 1.49)	1.01	(0.83, 1.23)	1.09	(0.93, 1.28)	1.28	(1.09, 1.51)
$100\sigma_d$			1.10	(0.71, 1.58)	0.98	(0.65, 1.44)			1.37	(0.93, 1.95)	1.50	(0.95, 2.26)

*Notes:* The estimation samples are 1984:Q1-2007:Q4 for the U.S. and 1981:Q1-1994:Q4 for Japan. We report posterior means and 90% credible intervals (5th and 95th percentile of the posterior distribution) in parentheses. All results are based on the last 50,000 draws from a RWMH algorithm, after discarding the first 50,000 draws. Entries with a \* indicate that we replaced the benchmark prior for this parameter with a tighter prior. See Online Appendix for further details.

## F Particle Filter For Sunspot Equilibrium

The particle filter is used to extract information about the state variables of the model from data on log output, log consumption-output ratio (for 4v specifications) inflation, and nominal interest rates over the periods 1984:Q1 to 2015:Q4 (U.S.) and 1981:Q1 to 2015:Q4 (Japan).

### F.1 State-Space Representation

Let  $y_t^o$  be the  $n \times 1$  vector of observables, where  $n$  is either 3 or 4. The vector  $x_t$  stacks the continuous state variables, which are given by  $x_t = [R_t, y_t, y_t^*, y_{t-1}, d_t, z_t, g_t, A_t]'$ , and  $s_t \in \{0, 1\}$ , is the Markov-switching process. Note that the output measures here are detrended by the level of technology  $A_t$  and only  $y_{t-1}$  is necessary for the growth specifications and  $y_{t-1}^*$  is necessary for the gap specifications.

$$y_t^o = \Psi(x_t) + \nu_t \quad (\text{A.17})$$

$$\mathbb{P}\{s_t = 1\} = \begin{cases} (1 - p_{00}) & \text{if } s_{t-1} = 0 \\ p_{11} & \text{if } s_{t-1} = 1 \end{cases} \quad (\text{A.18})$$

$$x_t = F_{s_t}(x_{t-1}, \epsilon_t) \quad (\text{A.19})$$

The first equation is the measurement equation, where  $\nu_t \sim N(0, \Sigma_\nu)$  is a vector of measurement errors. The second equation represents the law of motion of the Markov-switching process. The third equation corresponds to the law of motion of the continuous state variables. The vector  $\epsilon_t \sim N(0, I)$  stacks the innovations  $\epsilon_{z,t}$ ,  $\epsilon_{g,t}$ , and  $\epsilon_{R,t}$ . The functions  $F_0(\cdot)$  and  $F_1(\cdot)$  are generated by the model solution procedure. Measurement and state transition equations can be summarized by the densities  $p(y_t^o|x_t)$ ,  $p(s_t|s_{t-1})$ , and  $p(x_t|x_{t-1}, s_t)$ .

### F.2 Particle Filtering

Let  $\varsigma_t = [x_t', s_t']'$  and  $Y_{t_0:t_1}^o = \{y_{t_0}^o, \dots, y_{t_1}^o\}$ . Particle filtering relies on sequential importance sampling approximations. The distribution  $p(\varsigma_t|Y_{1:t}^o)$  is approximated by a set of pairs

$\{(\varsigma_t^{(j)}, W_t^{(j)})\}_{j=1}^M$  in the sense that

$$\frac{1}{M} \sum_{j=1}^N h(\varsigma_t^{(j)}) W_t^{(j)} \xrightarrow{a.s.} \mathbb{E}[h(\varsigma_t) | Y_{1:t}^o], \quad (\text{A.20})$$

where  $\varsigma_t^{(j)}$  is the  $j$ 'th particle,  $W_t^{(j)}$  is its weight, and  $M$  is the number of particles. Our implementation of the particle filters follows Algorithm 12 of Herbst and Schorfheide (2015). In the remainder of this section we provide a few implementation details.

**Measurement Errors.** The baseline measurement error standard deviations are as follows. Log output: 0.0016617; log consumption output ratio 0.0015; inflation 0.30560; interest rates 0.75056. We then reduce the baseline standard deviations by 0.7, 0.7, 0.7, and 0.2, respectively. For comparison, in our data set the standard deviations for output growth (not in percentages), the log consumption-output ratio, inflation, and interest rates are 0.011, 0.018, 2.02, 2.81 for Japan; and 0.006, 0.0098, 0.99, 3.01 for the U.S. To obtain the measurement error variance of inflation expectations, we scale the inflation measurement error variance by the ratio of the sample variances of inflation expectations and inflation in the data.

**Initialization.** The filter requires an initial distribution  $p(\varsigma)$ . Because we are operating under the assumption that the economies are in the targeted-inflation regime ( $s_t = 1$ ) at the beginning of the sample (and during the estimation period) and because in the relevant region of the state space the decision rules are well approximated by a first-order perturbation solution, we use the linear representation of the targeted-inflation equilibrium to construct an initial distribution.

Let  $t = 1$  correspond to the first observation in the sample. Because the law of motion for the detrended state variables (all elements of  $x_t$  except  $A_t$ ) is stationary, we can initialize the distribution in period  $t = 1$  using the implied ergodic distribution of the linearized system.  $A_1$  is treated as follows. We set  $\log A_1 = (\log Y_1 + \log Y_1^* - 2 \log y_*)/2$ , where  $y_*$  is the model implied steady state of  $Y_t/A_t$ . Conditional on  $\log A_1$  we can compute  $\log(Y_1/A_1)$  and  $\log(Y_1^*/A_1)$ . We treat these objects as “known,” setting their variance equal to zero. We then run the Kalman filter based on the observations  $y_2^o$  to  $y_4^o$  of the sample. We use the

posterior distribution of  $x_4|Y_{1:4}^o$  obtained from the Kalman filter iterations and  $s_4 = 1$  to initialize the nonlinear filter. In particular, we generate particles from  $p(\varsigma_4)$  by *iid* sampling. This initialization ensures that the model tracks the levels of  $Y_t$  and  $Y_t^*$ .

**Proposal Distribution.** States for the next period are drawn from the proposal distribution

$$g(\varsigma_t|\varsigma_{t-1}, y_t) = \begin{cases} g_0(x_t|x_{t-1}, y_t^o, s_t = 0)\lambda(\varsigma_{t-1}, y_t^o) & \text{if } s_t = 0 \\ g_1(x_t|x_{t-1}, y_t^0, s_t = 1)(1 - \lambda(\varsigma_{t-1}, y_t^o)) & \text{if } s_t = 1 \end{cases},$$

Rather than drawing  $x_t$  directly from a distribution, we draw the innovation  $\epsilon_t$  from a proposal distribution and then simulate the state-transition forward (see Algorithm 14 in Herbst and Schorfheide (2015)):  $\epsilon_t^{(j)} \sim N(\mu(s_t), \Sigma(s_t))$ . For  $\Sigma(s_t)$  we use the identity matrix and we determine  $\mu(s_t)$  by grid search, maximizing  $p(y_t^o|\bar{x}_{t-1}, y_t^o, \epsilon_t)p(\epsilon_t)$  with respect to  $\epsilon_t$ . Here  $p(\epsilon_t)$  is the DSGE model implied distribution of the shock innovations. Executing the grid search for each particle conditional on  $\bar{x}_{t-1}^{(j)}$  rather than the average across particles  $\bar{x}_{t-1}$  turned out to be too time consuming. We set  $\lambda(\varsigma_{t-1}, y_t^o) = 1/2$ .

**Number of Particles.** We set  $M = 100,000$ .